We are IntechOpen, the world's leading publisher of Open Access books
Built by scientists, for scientists

6,900
Open access books available

186,000
International authors and editors

200M
Downloads

Our authors are among the

154
Countries delivered to

TOP 1%
most cited scientists

12.2%
Contributors from top 500 universities

CLARIVATE ANALYTICS
BOOK CITATION INDEX
INDEXED

WEB OF SCIENCE™

Selection of our books indexed in the Book Citation Index
in Web of Science™ Core Collection (BKCI)

Interested in publishing with us?
Contact book.department@intechopen.com

Numbers displayed above are based on latest data collected.
For more information visit www.intechopen.com

Numerical Methods for Analyzing the Transients in Medium Voltage Networks

Dumitru Toader, Stefan Haragus and Constantin Blaj

Additional information is available at the end of the chapter

1. Introduction

The analysis of transient regimes in electric networks is a complex problem due to great number of elements, some nonlinear, as well as, due to the nonsinusoidal variation of currents and voltages. Numerical simulation can solve properly such a problem

There are available a lot of simulation programs for transients. One of the first of them, dedicated to electro energetic systems, was initiated by H.W.Dommel. Electromagnetic Transient Program (EMTP) was bought by Bonneville Power Administration (USA) (Dommel, 1995). Later on, from this initial program were developed several versions, such as MicroTrans, EMTP-RV, ATP (Alternative Transients Program), PSCAD (Chuco, 2005; DeCarlo & Lin, 2001).

Comparing some of the main simulation programs is not very conclusive, because each one of them are used in some versions trying to solve a large group of problems (Iordache & Mandache, 2004; Istrate et al., 2009).

Interface becomes more and more friendly, the library becomes larger and the facilities for creating own models are simpler to use. The speed of calculations and the storage capacity do no more represent a problem. It is possible now to implement some complicated algorithms able to solve problems with high speed in the variation of variables, able to solve all kinds of nonlinearities or to handle eigenvalues highly distanced one from another (large stiffness ratio dynamical systems).

An important criterion for the selection is represented by the integration of complex dynamical systems like rotating electric machines, relays, power electronic devices, FACTS, controllers etc. in the simulation. Some of the programs, depending on the way that were conceived, allow a better integration of these subsystems.

Choosing one or other of the simulation programs depends on the previous experience of the user, as well as, on the manner the program responds to the specific demands (Chuco, 2005; Danyek et al., 2002; Foltin et al., 2006; Karlsson, 2005; Rashid & Rashid, 2006).

No mater what program is used, the numerical analysis of transients eventually must be able to solve a set of differential – algebraic equations that models the physical system. By accounting the stage the numerical integration takes place at, there are two main classes of simulation programms.

One class consists of those programs that make the integration at element level, meaning that for each step of time discretization the differential equations associated to dynamic elements are transformed in finite difference relations. Several ways of approximation can be used, more frequently the trapeze rule being used. All these algebraic relations are then assembled and as a result an algebraic system of equations is obtained and consequently solved using specific algorithms. This procedure is repeated at each iteration step, the parameters involved in the equations being modified by the results obtained at the previous step. Usually the integration step is fixed, but if this is required by a lack of convergence, the integration step can be split in half and the computation process is resumed. This method is known under the name of the implicit integration method and is used in programs such as SPICE and EMTP (Blume, 1986).

A second class of programs uses a two step procedure. In the first step the mathematic model is expressed as a system of first order differential equations, known as the system's state equations. During the next step this system of equations is integrated using algorithms with fixed step or with variable steps, depending on the systems particularities. The advantage of this method, called the state variables method, is to treat in the same way, in a unitary manner, electric networks, electric machines, drives, control devices or any other device that allows state equations. A representative of this method is SimPowerSystems™ which is an extension of Simulink® with tools for modeling and simulating of electrical power systems. It provides models of many components used in these systems, including three-phase machines, electric drives, and libraries of application-specific models such as Flexible AC Transmission Systems (FACTS) and wind-power generation. Harmonic analysis, calculation of Total Harmonic Distortion (THD), load flow, and other key power system analyses are automated (Mathworks®).

The precision of the results obtained by integration of the equations describing the simulated system is quite remarkably high. It is obvious that none of the simulation programs, no mater which of the methods is using, cannot be more precise than the mathematic models used for the simulated components. The accuracy of the values of the parameters of these models is of high importance.

2. The state-variable method for electrical circuits

Medium voltage electric networks are in fact complex circuits mainly made of power sources, resistors, inductors, capacitors and, sometimes, other electric components.

Analyzing transient regimes in such networks is the same as the analysis of any other complex electric circuit (Dessaint, et al. 1999; Mandache & Topan, 2009; SIMULINK, 1997).

Generally, an electric circuit, no mater how complex it is, is described by an algebraic linear system of equations, obtained by applying the Kirchhoff's laws. This system of equations reflects the circuit's topology. To complete the model, the voltage-current equation at the terminals of each element of circuit (called also constitutive relations) must be added.

The inductors and the capacitors are described by constitutive relations in which are involved the derivatives of currents, respectively voltages. As a result, the mathematic model of an electric circuit consists of a system of algebraic and differential equations (DAE).

In the electric circuit theory it is demonstrated that each current or voltage can be expressed as function of inductors currents and capacitors voltages. By other words if the inductors currents and the capacitors voltages are known, all remaining currents and voltages are uniquely determined and because of this they are called state-variables.

The state-variable equations are obtained by elimination of the algebraic equations in the initial DAE.

The modelization of an electric circuit made using state-equations has several important advantages.

First of all, electric circuits can be integrated with other dynamic systems, of completely different physical nature, as long as the last ones are described also by state-equations.

By the other hand, the procedures for integrating state-equations have a well-established theoretic support, being the domain of interest for quite a long period of time for famous mathematicians.

Finally, but not last, the method can be applied to linear circuits, as well as, to nonlinear circuits.

Of course there is a price to be paid for all these advantages: a certain difficulty in the elimination of the algebraic equations from the system.

In order to give an example for the basics of the state-variable method, we will analyze the simple RLC series connection circuit supplied by an ideal voltage source $u(t)$. The Kirchhoff equations and the constitutive relations for such a circuit are, respectivelly:

$$
\begin{aligned}
& i_R(t) = i_L(t) = i_C(t), \\
& u(t) = u_R(t) + u_L(t) + u_C(t), \\
& u_R(t) = Ri(t), \\
& u_L(t) = L\frac{di_L(t)}{dt}, \\
& i_C(t) = C\frac{du_C(t)}{dt}.
\end{aligned}
\tag{1}
$$

It is customary to write the last two equation in the form

$$\frac{di_L(t)}{dt} = \frac{1}{L} u_L(t),$$
$$\frac{du_C(t)}{dt} = \frac{1}{C} i_C(t).$$

(2)

With the remaining equations $u_L(t)$ and $i_C(t)$ are obtained as functions of $i_L(t)$, $u_C(t)$:

$$u_L(t) = u(t) - R i_L(t) - u_C(t),$$
$$i_C(t) = i_L(t).$$

(3)

By the substitution in (2) it follows

$$\frac{di_L(t)}{dt} = \frac{1}{L} u(t) - \frac{R}{L} i_L(t) - \frac{1}{L} u_C(t),$$
$$\frac{du_C(t)}{dt} = \frac{1}{C} i_L(t),$$

(4)

or, in matrix form,

$$\frac{d}{dt}\begin{bmatrix} i_L(t) \\ u_C(t) \end{bmatrix} = \begin{bmatrix} -\dfrac{R}{L} & -\dfrac{1}{L} \\ \dfrac{1}{C} & 0 \end{bmatrix}\begin{bmatrix} i_L(t) \\ u_C(t) \end{bmatrix} + \begin{bmatrix} -\dfrac{1}{L} & 0 \end{bmatrix}\begin{bmatrix} u(t) \\ 0 \end{bmatrix}.$$

(5)

This is a first order differential equations system, with the variables $i_L(t)$ and $u_C(t)$.

If the initial conditions $i_L(0)$ and $u_C(0)$ are known, then, according to the uniqueness theorem for the solution of a first order differential equation, the solution $i_L(t)$ and $u_C(t)$, $t≥0$, exists and is unique.

Once the solutions for the variables $i_L(t)$ and $u_C(t)$ are available, immediately all the other unknowns are solved. Therefore, $i_L(t)$ and $u_C(t)$ are the state-variables of the circuit, and (5) is the matrix state equation of the circuit.

Generally, for a linear electric circuit, the matrix state equation is of the type (6):

$$\frac{d\mathbf{x}(t)}{dt} = \mathbf{A}\,\mathbf{x}(t) + \mathbf{B}\,\mathbf{u}(t),$$

(6)

where $x(t)$ is the column matrix of the inductor currents and of the capacitor voltages (state-vector),

$u(t)$ is the column matrix of independent supply sources (sources vector), and, A and B are matrix depending on the circuits topology and of its parameters.

The total number of the state variables is equal with the sum of the number of the inductors and capacitors from the circuit, representing the order of the circuit.

All the other unknown variables are represented by the column matrix $y(t)$ (also called output vector) represented by a linear combination of the state-vector and the sources vector):

$$\mathbf{y}(t) = \mathbf{C}\mathbf{x}(t) + \mathbf{D}\mathbf{u}(t), \tag{7}$$

C and D being matrix of the same origin as A and B.

The equation given by (6) describes the model, in state-space, of a linear electric circuit.

It is possible, as the result of using ideal elements in the modelization, to occur capacitive loops or inductive sections.

(a)

(b)
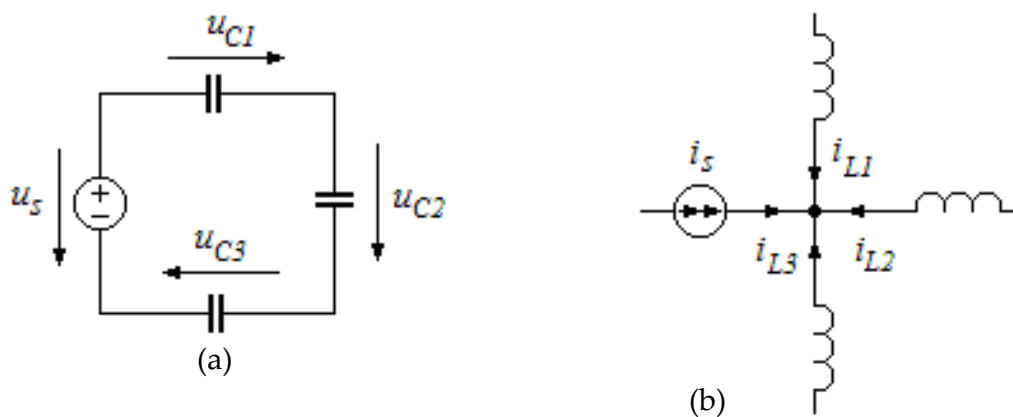
Figure 1. Capacitive loop and, respectively, inductive section

A capacitive loop (see Fig. 1a) is a loop consisting only from capacitors and, possibly, independent voltage sources.

In this case the voltages at the terminals of capacitors from the loop are no more linearly independent variables, because the second Kirchhoff's law gives:

$$-u_S + u_{C1} + u_{C2} + u_{C3} = 0. \tag{8}$$

One, arbitrarily selected, of the capacitor voltages can be expressed as a linear combination of the other voltages.

Such a situation is present also for inductive sections.

An inductive section is represented in Fig.1b, being composed by the convergence in a node of ideal inductors and, possibly, independent current sources. In this case the first Kirchhoff's law states that

$$-i_S + i_{L1} + i_{L_2} + i_{L_3} = 0. \tag{9}$$

Again anyone of the state variables can be expressed as a function of the others.

The order of an RLC circuit , meaning the number of linearly independent variables (and by consequence the number of state-equations) is equal to $n_{LC} - n_{bC} - n_{sL}$:

n_{LC} is the total number (sum) of inductors and capacitors

n_{bC} is the number of the capacitive loops

n_{sL} is the number of inductive sections.

The programs performing the analysis make the detection of capacitive loops and of the inductive sections presents in the electric circuit. Usually, it is recommended to introduce a very small value resistor in series connection with one of the elements of the capacitive loop, or to connect a high value resistor in parallel to one of the elements of the inductive section. By this the circuits differs from the original, but the difference in currents values and voltages values are insignificant

The method of state variables can be naturally extended for nonlinear circuits. In this case the circuit equations are of the form

$$f_R\left(u_R, i_R\right) = 0,$$
$$u_C = \frac{dq}{dt} \, ; \, f_C(u_C, q) = 0, \tag{10}$$
$$i_L = \frac{d\Phi}{dt} \, ; \, f_L(i_L, \Phi) = 0,$$

with f_R, f_C, f_L being the characteristics of nonlinear elements and, q and Φ, the electric charge of the capacitor, respectively the magnetic flux trough the inductor.

The procedure for obtaining the state equations is similar as for linear circuits, with the difference that the state variables are q and Φ. These variables are present in the dynamic constitutive equations.

The variables u_C and i_L are obtained as functions of q and Φ and afterwards :

$$\frac{d\boldsymbol{x}}{dt} = \boldsymbol{F}\left(\boldsymbol{x}, t\right), \tag{11}$$

In (11) x is the column matrix of state variables (state vector), and F is a matrix depending on the circuits topology and on the nonlinear characteristics.

If for linear circuits, the circuits equations can be always reduced to state equations, for certain nonlinear circuits it is not possible to allow state equations (Hasler & Neirynck, 1985).

Anyhow, for a modelization not excessively idealized and a reasonable choice of state variable it is possible to obtain always state equations. For nonlinear state equations even the problem of existing or not of a solution might occur.

State equations for linear circuits have exact analytically determined solution, available in any book of college mathematics. If the order of the circuit is higher than three, analytic solution implies calculations so complicated that this method becomes inefficient. For this kind of situations a large offer of numeric integrations methods is available embedded in the commercial programs of numeric simulation.

3. Simulation of electric circuits using PSPICE

The levels of the analysis of electric circuits performed by PSPICE are, mainly, the following (Radoi, 1994; Vladimirescu, 1999):

a. Solving a linear electric circuit, invariable with time,
b. Solving a nonlinear electric circuit,
c. Solving a time variable electric circuit.

For solving the electric circuit problems PSPICE uses the branch current method. Each element of the circuit is considered being placed between two nodes. The nodes are numbered from "0", the reference node, to N and the position of an element is given by the numbers of its terminals. A very simple circuit example is given in Fig. 2.
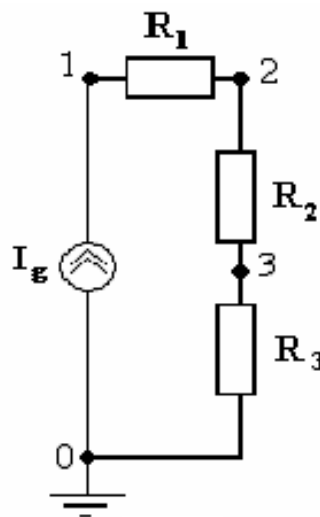
Figure 2. Simple circuit for SPICE application

$$\begin{cases} \dfrac{V_0 - V_3}{R_3} = -I_g & \text{for node 0,} \\[2mm] \dfrac{V_1 - V_2}{R_1} = I_g & \text{for node 1,} \\[2mm] \dfrac{V_1 - V_2}{R_1} = \dfrac{V_2 - V_3}{R_2} & \text{for node 2,} \\[2mm] \dfrac{V_2 - V_3}{R_2} = \dfrac{V_3 - V_0}{R} & \text{for node 3.} \end{cases} \tag{12}$$

These equations can be written in matrix form also as (13), where $[\,I\,]$ is the column matrix of the sources for all the nodes, in the same order as the unknown nodes potentials in matrix $[\,V\,]$. $[\,G\,]$ is the square conductance matrix.

The potential of the reference node, "0", is taken with "zero" value so all the other N-1 nodes potentials remain as unknown values in the equation system.

With $V_0 = 0$, system (13) is transformed into a system (14) with N-1 equations.

In this very simple example remain only 3 unknown values of nodes potentials (14).

$$
\begin{bmatrix} -I_g \\ +I_g \\ 0 \\ 0 \end{bmatrix} =
\begin{bmatrix}
\dfrac{1}{R_3} & 0 & 0 & -\dfrac{1}{R_3} \\[2mm]
0 & \dfrac{1}{R_1} & -\dfrac{1}{R_1} & 0 \\[2mm]
0 & -\dfrac{1}{R_1} & \dfrac{1}{R_1}+\dfrac{1}{R_2} & -\dfrac{1}{R_2} \\[2mm]
-\dfrac{1}{R_3} & 0 & -\dfrac{1}{R_2} & \dfrac{1}{R_2}+\dfrac{1}{R_3}
\end{bmatrix}
\cdot
\begin{bmatrix} V_0 \\ V_1 \\ V_2 \\ V_3 \end{bmatrix}
\quad \text{or,} \quad [\,I\,]=[\,G\,]\cdot[\,V\,] \tag{13}
$$

$$
\begin{bmatrix} +I_g \\ 0 \\ 0 \end{bmatrix} =
\begin{bmatrix}
\dfrac{1}{R_1} & -\dfrac{1}{R_1} & 0 \\[2mm]
-\dfrac{1}{R_1} & \dfrac{1}{R_1}+\dfrac{1}{R_2} & -\dfrac{1}{R_2} \\[2mm]
0 & -\dfrac{1}{R_2} & \dfrac{1}{R_2}+\dfrac{1}{R_3}
\end{bmatrix}
\cdot
\begin{bmatrix} V_1 \\ V_2 \\ V_3 \end{bmatrix} . \tag{14}
$$

The system (14) can be solved using the Gaussian elimination method (Ross, 2004).

An equivalent method that can be used for solving the system is the LU factorization, by decomposing the [G] matrix.

Matrix [G]=[L]·[U], with [L] being a matrix with "1" on the principal diagonal, and [U] is a matrix having only "0" below the principal diagonal. This method is more advantageous than the "classic" Gauss elimination method, mainly when the equation [I] = [G]·[V] has to be solved several times: several sources [I] for the same conductance matrix. This is the situation for solving our problem using PSPICE, so that the LU factorization method shall be used.

In the analysis of dynamical circuits either the sources, voltage or current sources, have time variation, either the topology of the circuit is changing. If the passive elements are resistors, linear or nonlinear, using a time step Δt for the discretization of the time variation (sinusoidal, exponential, linear) of the sources. For each time moment a set of values [V(t)] is calculated and memorized. These values can be used in further graph representations or printed.

The presence of inductors and/or capacitors implies replacing them with equivalent elements.
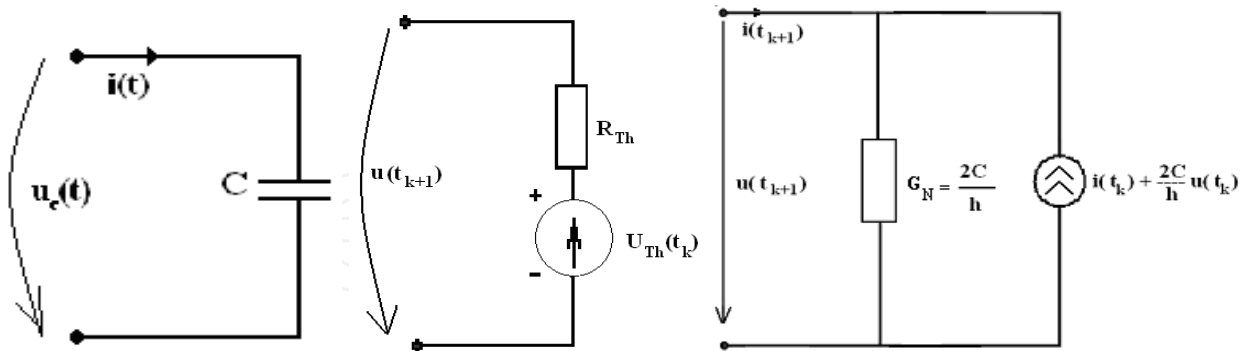
Figure 3. Thevenin and Norton generators for a capacitor , when trapeze method is used

For an iterative calculation process the capacitor can be replaced by a Thevenin or a Norton generator. The Norton generator presented in the Fig. 3 has the parameters calculated according to the trapeze method of integration. The method using the Euler's regressive algorithm and the Gear's second order algorithm can be used also, but the equivalences (parameters of the Norton or Thevenin generators) are different from those presented in Fig. 3.
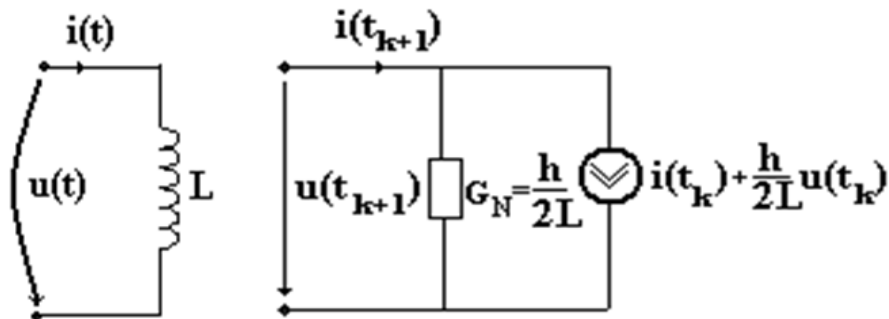
Figure 4. Norton equivalent generator representation of a inductor, when trapeze method is used

In a similar manner for an inductor can be used a Norton equivalent generator or a Thevenin equivalent generator, with parameters depending on the method used for solving the problem. Taking the nodes potentials as unknown values it is more suitable to use the Norton generator equivalent to the inductor in a dynamic circuit.

The transient regime analysis is the most important analysis that can be performed using PSPICE.

When the transient regime begins with non zero initial conditions this fact can be introduced in the program by the option UIC (use initial conditions).

The situation of the modelization of a complex network is shown in the Fig. 5.

The transient regime is triggered by closing the switch, meaning that phase one is grounded, as if a fault phase to ground is produced.

Resistor R$_{17}$ has a value that is corresponding to the conditions of the fault.
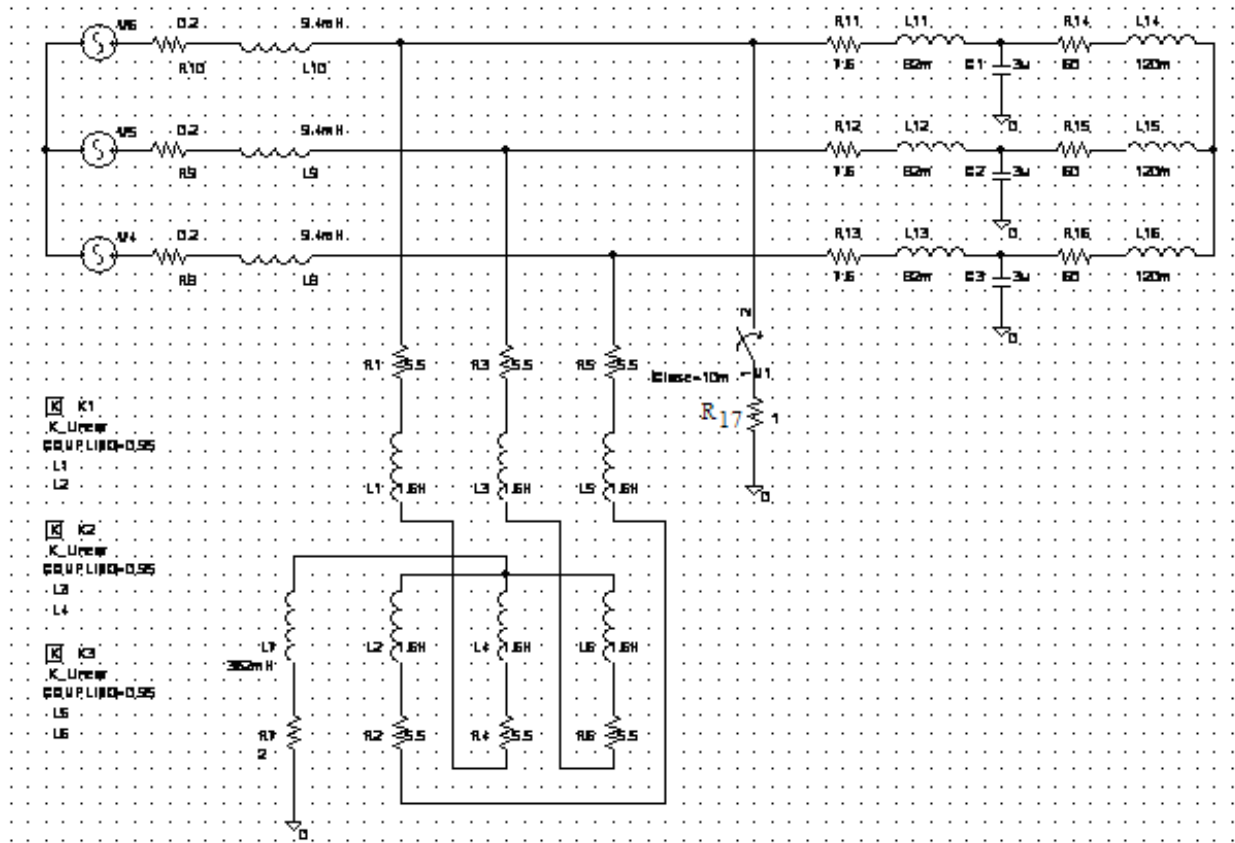
Figure 5. MVN represented as a complex circuit in SPICE drawing

Currents and voltages can be represented, as on a "soft" oscilloscope, after solving the transient regime, using the elements of the V[t] matrix, calculated for each time step, and the resulting, calculated, currents values.
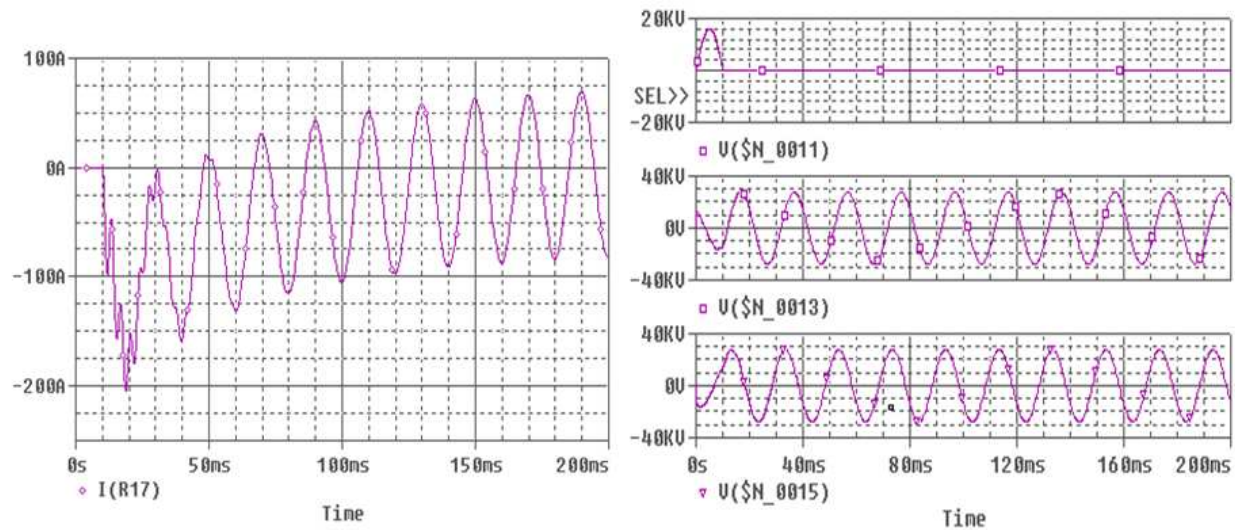
Figure 6. Current and voltages representation as SPICE output oscillogrames

4. Numeric simulation of transients triggered by faults in medium voltage networks

Faults in medium voltage networks (MVN) generate transient regimes with duration depending on the networks parameters, on the contact type at the fault place and on the default type itself. The numeric simulation performed in this chapter is based on PSPICE and the transient regimes are caused by simple and double grounding faults, as well as, by the fault produced by a broken conductor, grounded towards the consumer. A fault of the type broken conductor grounded towards the source can be treated similar as the simple grounding fault, with an insignificant error, so shall be no more analyzed in the followings (Sybille et al., 2000).

The elements that are important in the analysis are:

- the initial phase α of the faulty phase,
- the electric resistance at the fault, grounding point,
- the method used for grounding the neutral of the network,
- the functioning regime of the MVN.

4.1. The structure of MVN

The single line diagram of the MVN whose behavior is studied in case of transient caused by faults is presented in Fig. 7.
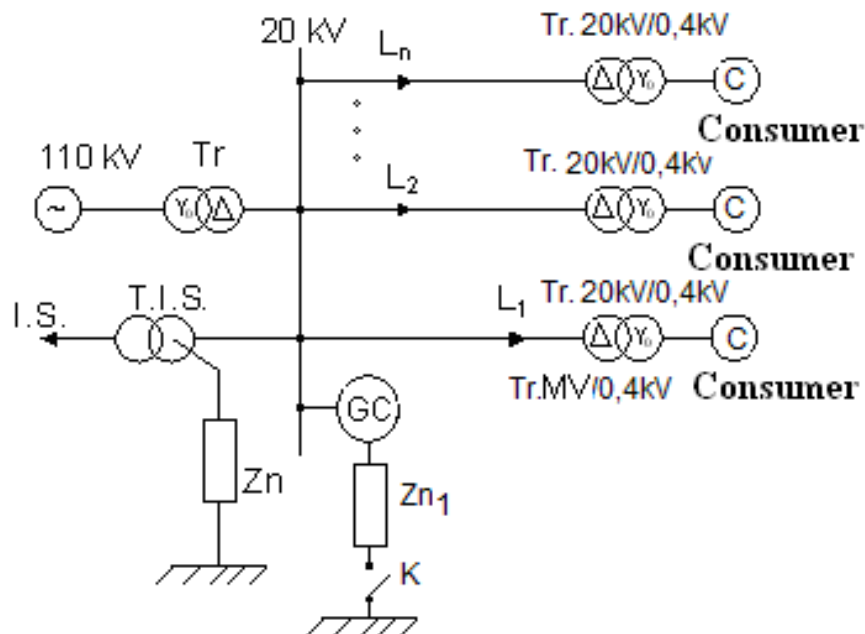
Figure 7. Single Line Diagram of the MVN

The MVN in Fig. 7 contains the following elements:

- The source, the 110kV line supplying the transformer 110kV/20kV, considered as being of infinite power supply and internal impedance zero,

- The transformer (Tr) 110kV/20kV star connection with neutral point on 110kV side and delta connection on the 20kV side,
- The lines of 20kV (L_1 ... L_n),
- The transformers TR.20kV/0.4kV supplying low voltage consumers, transformers having star or delta connection on the 20kV side and star with null or zigzag with null on the low voltage side,
- Low voltage consumers (C),
- The transformer for internal services (TIS) ; this transformer is used also for creating the artificial null of the 20kV network (has zigzag connection with null on the 20kV side and star with null on the low voltage side),
- The grounding inductor (GC) , having zigzag with null and creates the artificial null of the 20kV network,
- The impedance for treatment of the null (Z_n), impedance that might be a compensation inductor, a resistor or might be missing in the case of isolated null,
- The resistor for the null's treatment (Z_{n1}),
- The switch for the connection to the ground of the resistor Z_{n1}.

The model is designed with the possibility of changing the values of parameters.

4.2. Numerical simulation of some fault types

The numeric simulator of the three phased circuit corresponding to a MVN is shown in Fig.8. The PSPICE program is used to perform the modelization. Several types of faults are simulated using the model:

- simple grounding fault,
- double grounding fault,
- broken conductor and grounded on the consumer side.

The MVN where the faults are modelized has the following characteristics:

- nominal line voltage 20kV,
- S = 25MVA, the apparent power of the transformer 110kv/MV,
- the capacitive current of the MVN is 100A,
- the current of the two faulty lines , 8A each,
- the apparent power of the consumers is 80% of the nominal one and is uniformly distributed on the MV lines.

The simulator contains three lines, denoted with "a", "b" and "c" , so that to each index of parameter such as resistance or inductance is added a, b or c. The line "c" is considered as the healthy line and is the equivalent of all the 20kV lines without fault (Bucatariu et al., 2009; Drapela, 2009)

The line "a" is provided with the possibility of the simulation of a simple grounding fault, by connecting Vs_a. The same line "a" might simulate a fault of the type broken conductor (by opening the switch VSGOL). Even more, by opening the switch VSGOL and closing, in

the same time, the switch VS$_a$ it is possible to simulate a fault of the type broken conductor and grounded on the consumer's side.

The line "b" can simulate a simple grounding fault by closing the switch VS$_b$.

The fault of the type double grounding is simulated by closing the switch VS$_a$ connected to the line "a" and closing the switch VS$_b$ connected to the line "b", as well.

If a fault of the type double grounding on the same line is wanted to be simulated, the switch VS$_b$ should be moved from line "b" to line "a".

The parameters of the Earth (resistance, inductance) are encompassed in the parameters of the electric line.
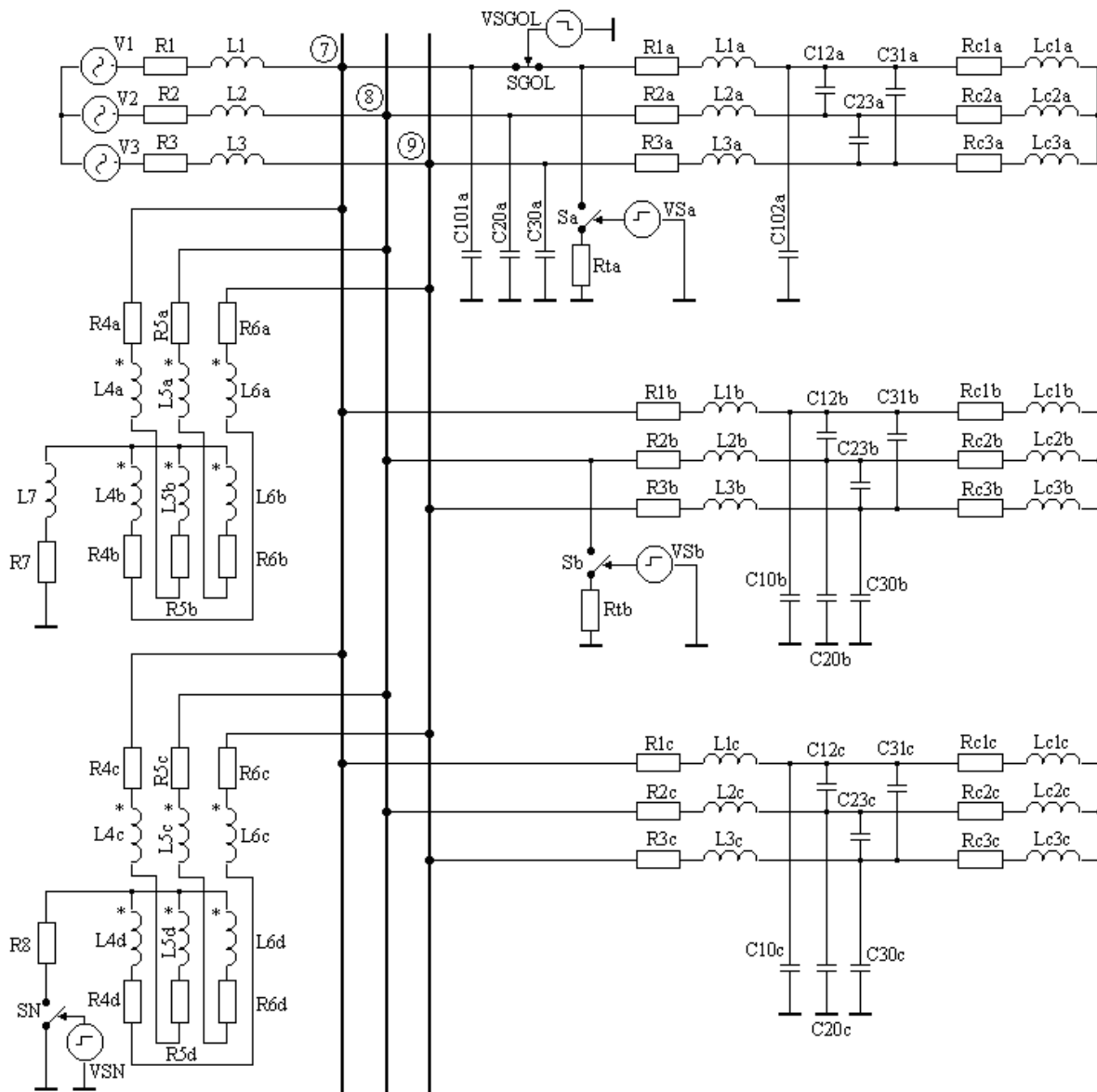
Figure 8. Three phased circuit simulating a MVN

4.2.1. The single phase-to-ground fault

Using the numerical simulator a multitude of situation could be analyzed.

One of those situations is the one when the MVN has the null grounded trough compensation inductor and the MVN functions under resonance conditions, respectively overcompensated 10%.

In these circumstances the evolution of voltages and currents during the transient is analyzed according to:

- the initial phase of the faulty phase (α) in the very moment when the fault is produced
- the electric resistance at the fault place (R_t)
- the way the null is treated
- the functioning regime (resonance, under or over compensated)

The first oscillogram, left side, is corresponding to the currents and the second corresponding to the voltages.

In these oscillograms I(S) represents the time variation of the current at the fault place, the zero sequence current of the faulty line is denoted as (I(R1a)+I(R2a)+I(R3a))/3, the zero sequence current is (I(R1b)+I(R2b)+I(R3b))/3 on the healty line, and the current trough the element for grounding the neutral point is I(L7).

In the oscillograms of the voltages , V(7), V(8) and V(9) represent, respectively, the voltages of the three phases and the zero sequence voltage of the MVN bars is represented by (V(7) + V(8) + V(9))/3.

In figures 9....20 the results correspond to the 10% overcompensated MVN with the neutral point grounded with compensation inductor. Only two values, 0 and 90°, of the initial phase of the voltage of the faulty line are taken into account. An intermediate value of 45° for this angle does not modify significantly the transient of the simple grounding fault.

From the oscillograms it can be observed that the initial phase of the faulty phase has great importance in the evolution of voltages and currents during the transient regime caused by the simple gounding fault.

Knowing, as accurate as possible, the evolution in time of the voltages gives the possibility of a good design for the MVN, strong enough to resist to the maximal applied voltage.

The maximal values of the currents are important for the correct evaluation of the mechanical forces acting on lines conductors, on the insulators and on the bars of MVN from the transformer station 110kV/MV.

The way that the electric contact is established, R_t , at the fault place, is very important in the transient evolution of the voltages and currents. If the resistance is over 100Ω the transient vanishes rapidly, in less than 5ms, and the maximal values of voltages and currents are not significant. This conclusion results by comparing oscillograms from Fig. 9 to Fig. 19, and, respectively, from Fig. 10 to Fig. 20.
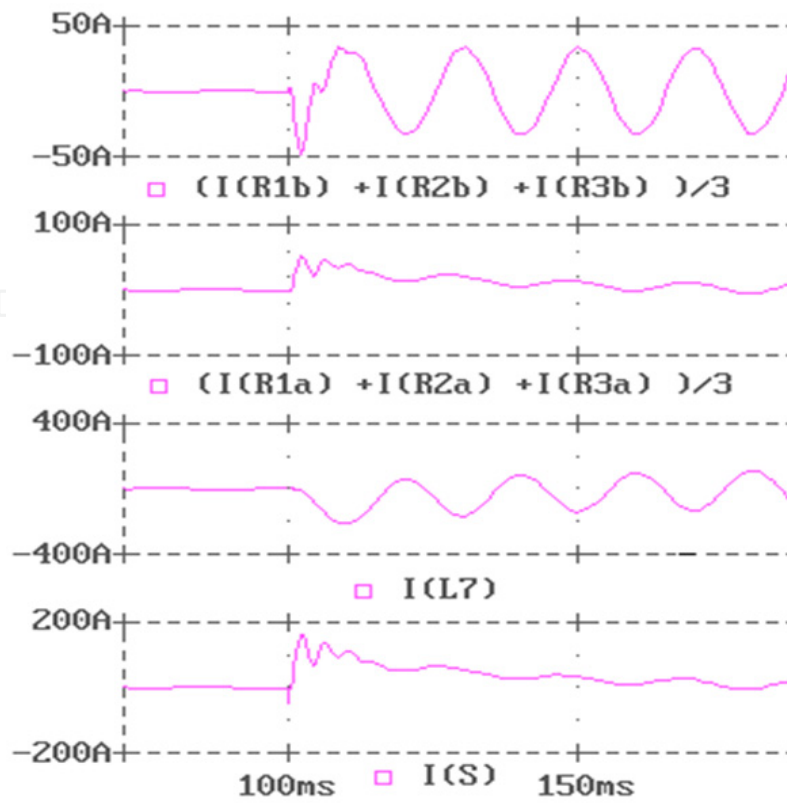
Figure 9. Time variation of the currents when MVN is 10% overcompensated and $R_t = 1\Omega$, $\alpha = 0°$
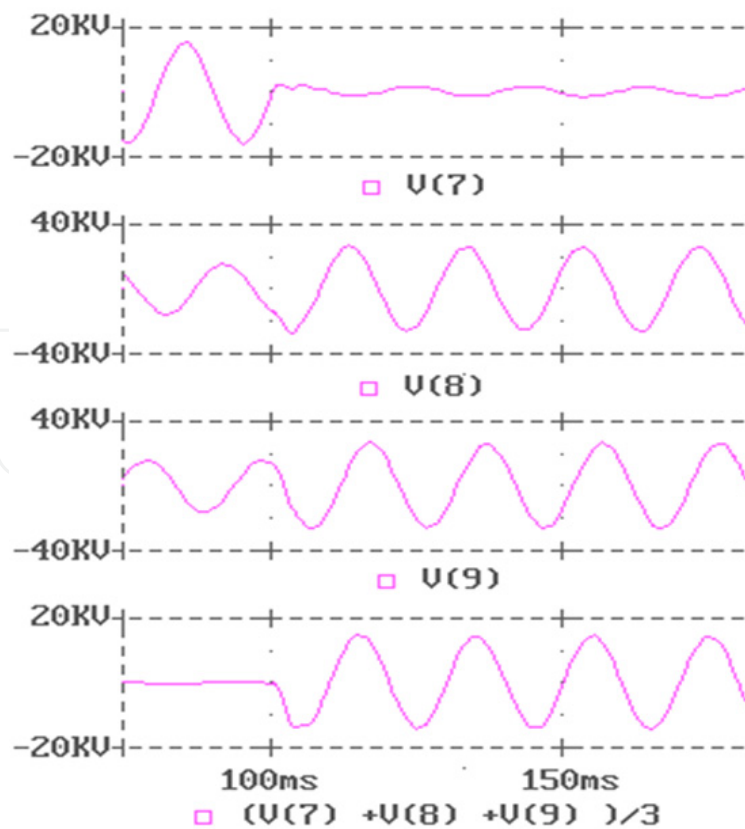
Figure 10. Time variation of the voltages when MVN is 10% overcompensated and $R_t = 1\Omega$, $\alpha = 0°$
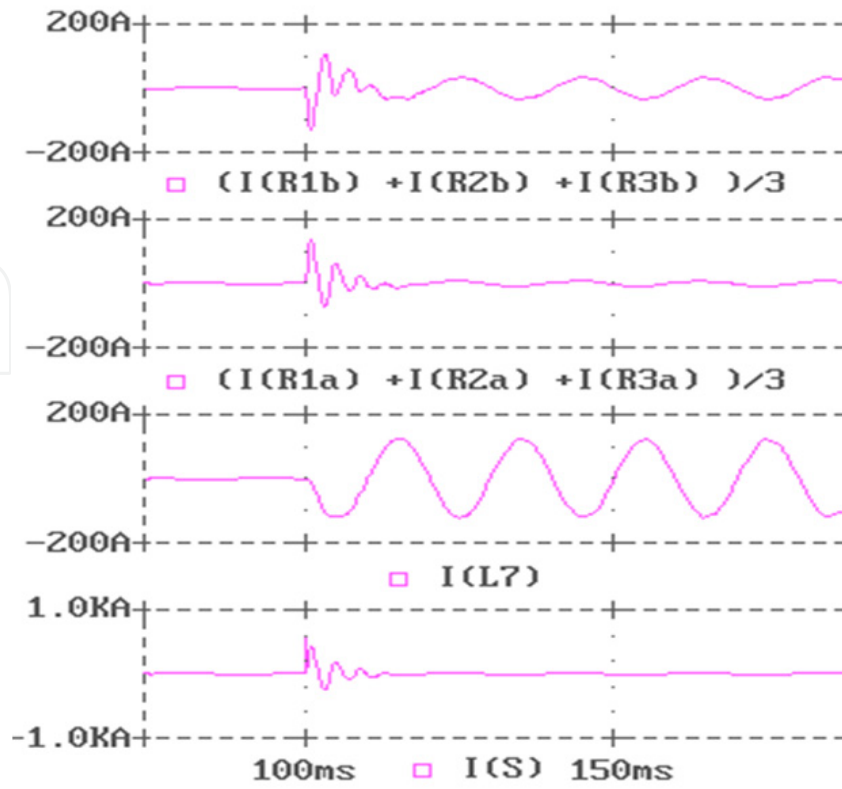
**Figure 11.** Time variation of the currents when MVN is 10% overcompensated and $R_t = 1\Omega$, $\alpha = 90°$
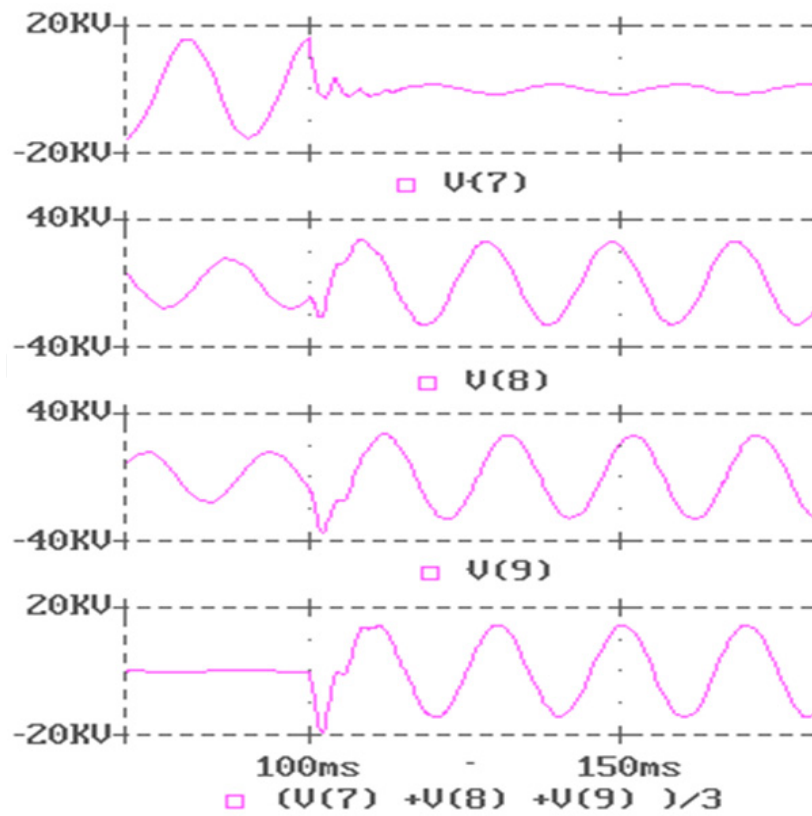
Figure 12. Time variation of the voltages when MVN is 10% overcompensated and $R_t = 1\Omega$, $\alpha = 90°$
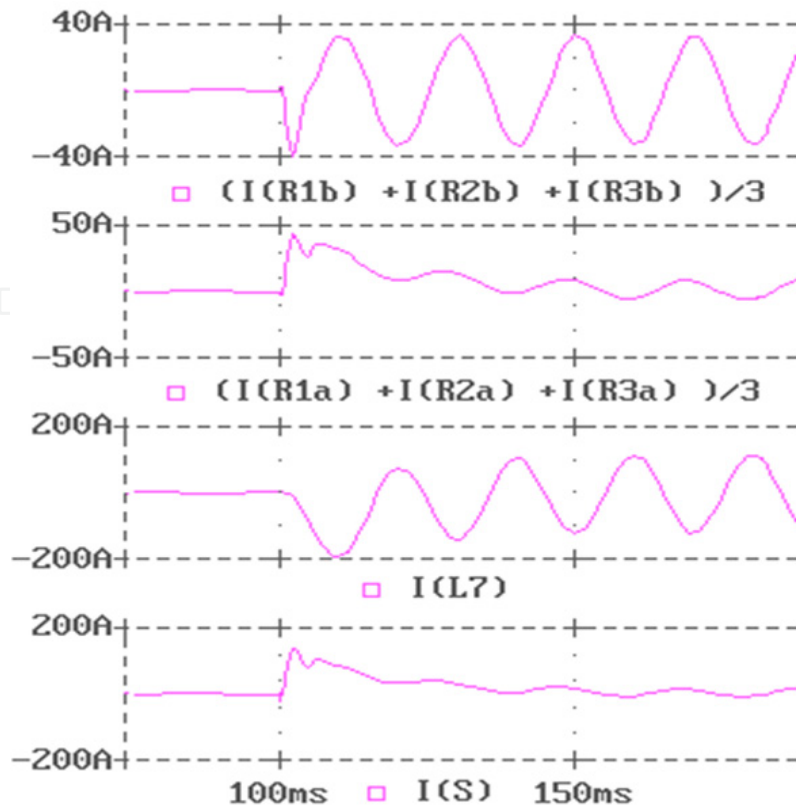
Figure 13. Time variation of the currents when MVN is 10% overcompensated $R_t = 10\Omega$, $\alpha = 0°$
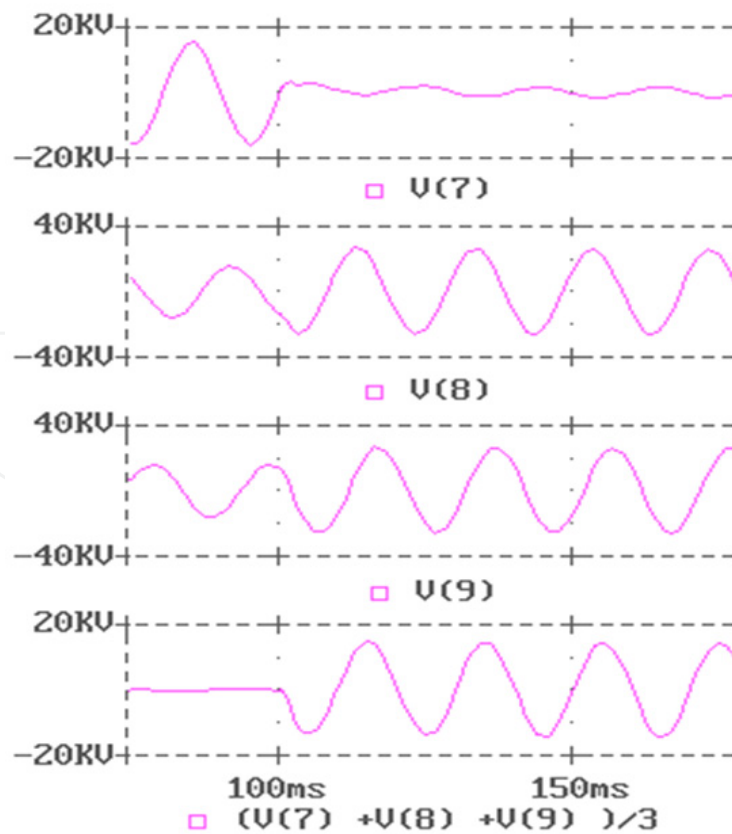
Figure 14. Time variation of the voltages when MVN is 10% overcompensated and $R_t = 10\Omega$, $\alpha = 0°$
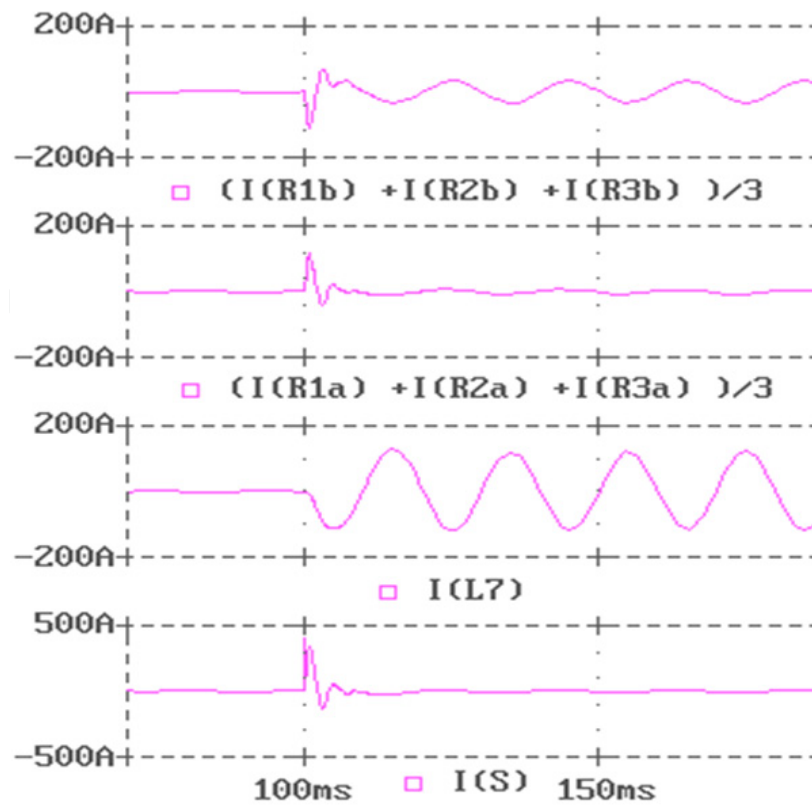
Figure 15. Time variation of the currents when MVN is 10% overcompensated $R_t = 10\Omega$, $\alpha = 90°$
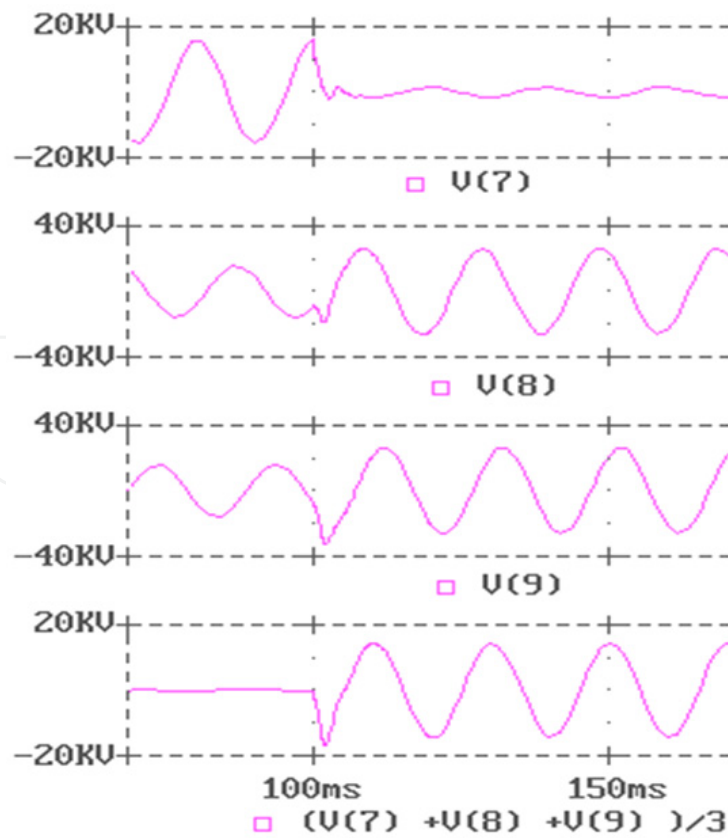
Figure 16. Time variation of the voltages when MVN is 10% overcompensated and $R_t = 10\Omega$, $\alpha = 90°$
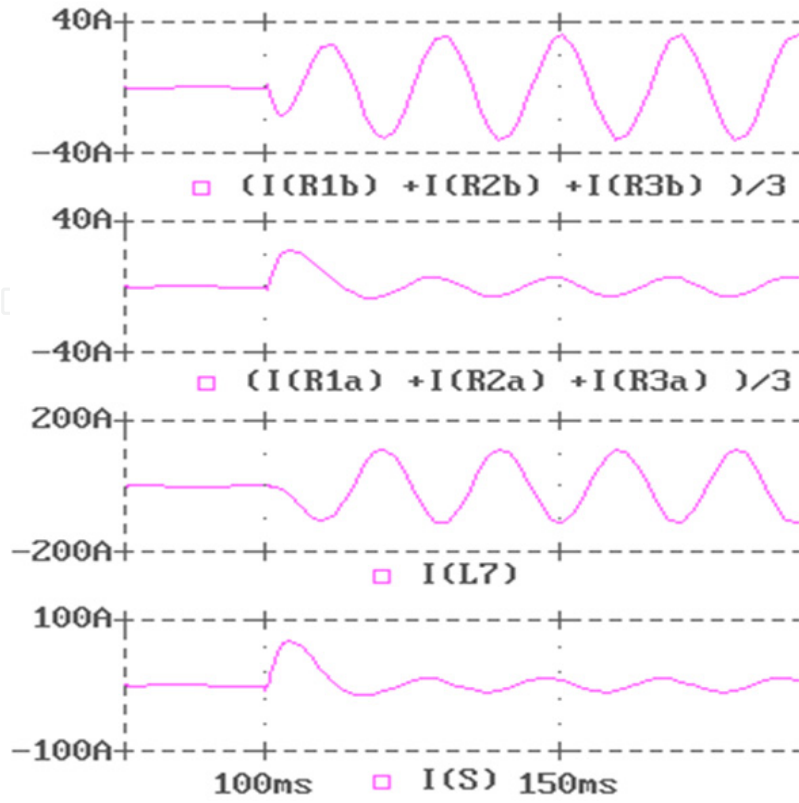
Figure 17. Time variation of the currents when MVN is 10% overcompensated $R_t = 100\Omega$, $\alpha = 0°$
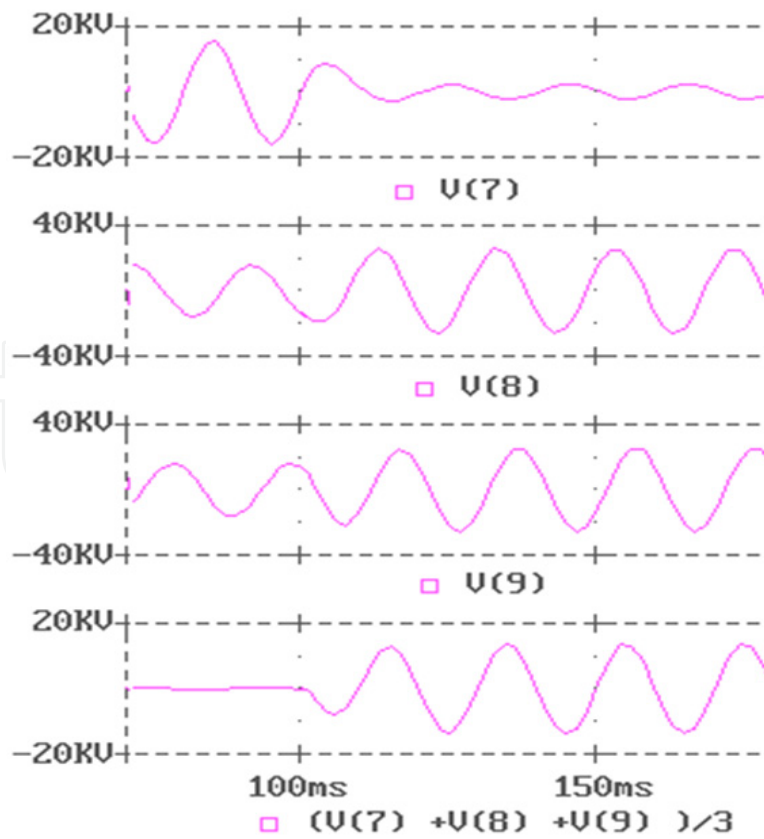
Figure 18. Time variation of the voltages when MVN is 10% overcompensated and $R_t = 100\Omega$, $\alpha = 0°$
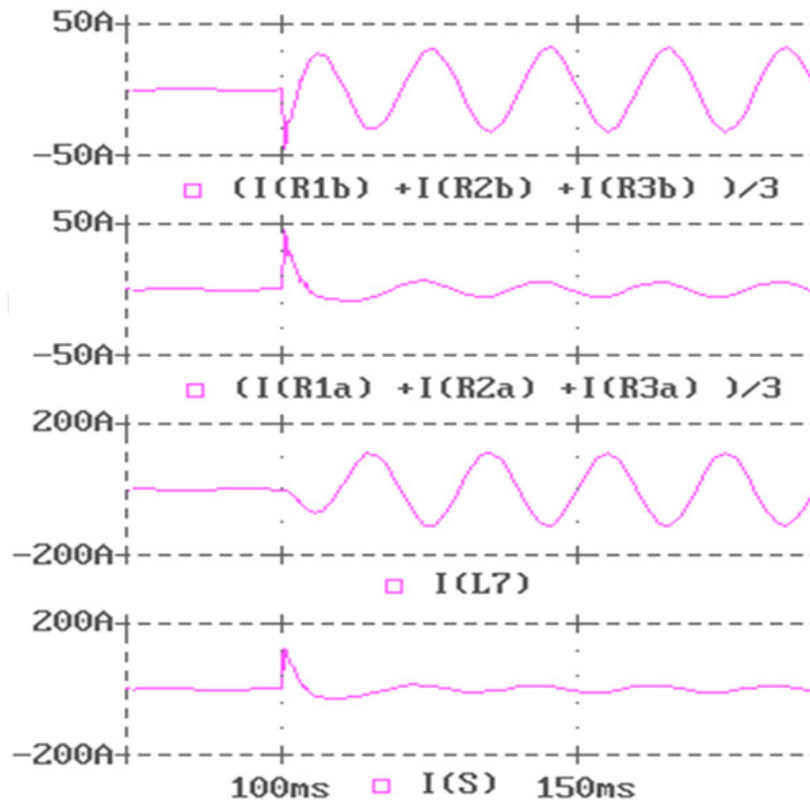
Figure 19. Time variation of the currents when MVN is 10% overcompensated $R_t = 100\Omega$, $\alpha = 90°$
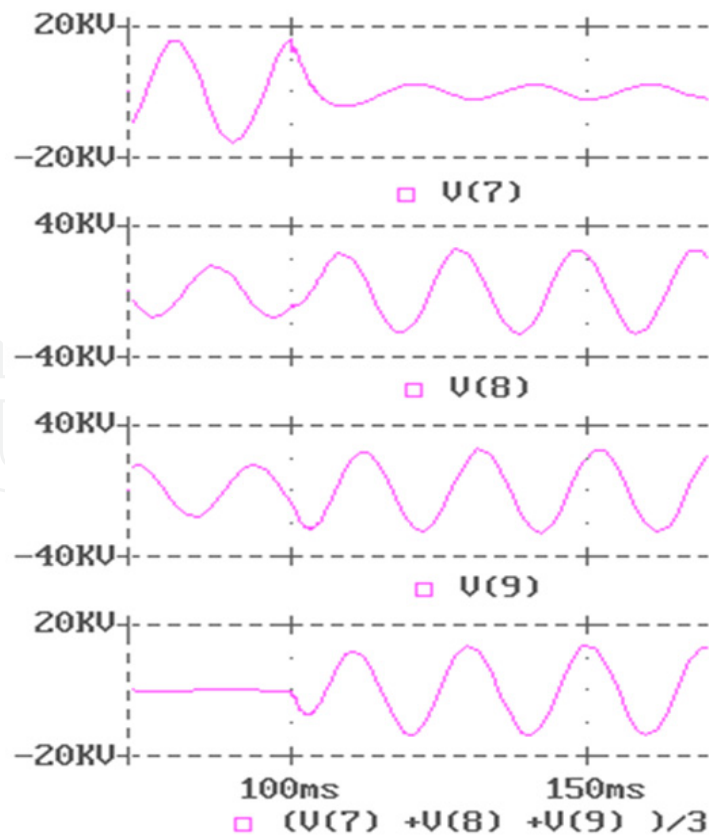
Figure 20. Time variation of the voltages when MVN is 10% overcompensated and $R_t = 100\Omega$, $\alpha = 90°$

If the MVN is functioning at resonance, the same simulation results are presented and, in addition, also the 45° value for the initial phase of the faulty phase voltage is presented.

The oscillograms show that the differences between the 10% overcompensated regime and the resonant regime are not significant.

If the functioning regime is far from being at resonance the transient regim produced by simple grounding fault is very short and the variation of voltages and currents is less important.

The maximal value of the current at fault place is obtained for 90° (comparing α values 0°, 45°, respectively 90°).

For $R_t = 1\Omega$ at $\alpha = 45°$ the current is twice its value at 0° and at 90° the current at the fault place is four times greater than the same current if $\alpha = 0°$.

If R_t becomes 10Ω the conclusions regarding the dependence of the current at the fault place on the phase α remain the same (higher α, higher value of the current) but with a decrease of about 25% of the maximal value of the current for a 10 times increase of the resistance at the fault place.
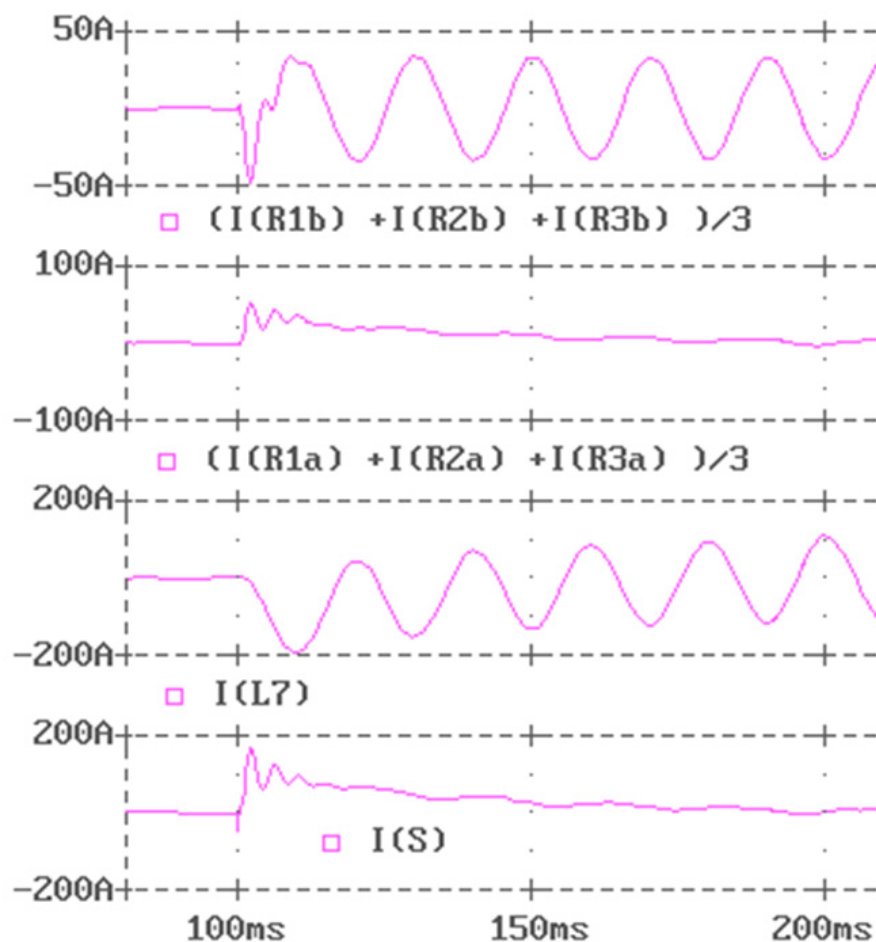

**Figure 21.** Time variation of the currents when MVN is at resonance , $R_t = 1\Omega$, $\alpha = 0°$
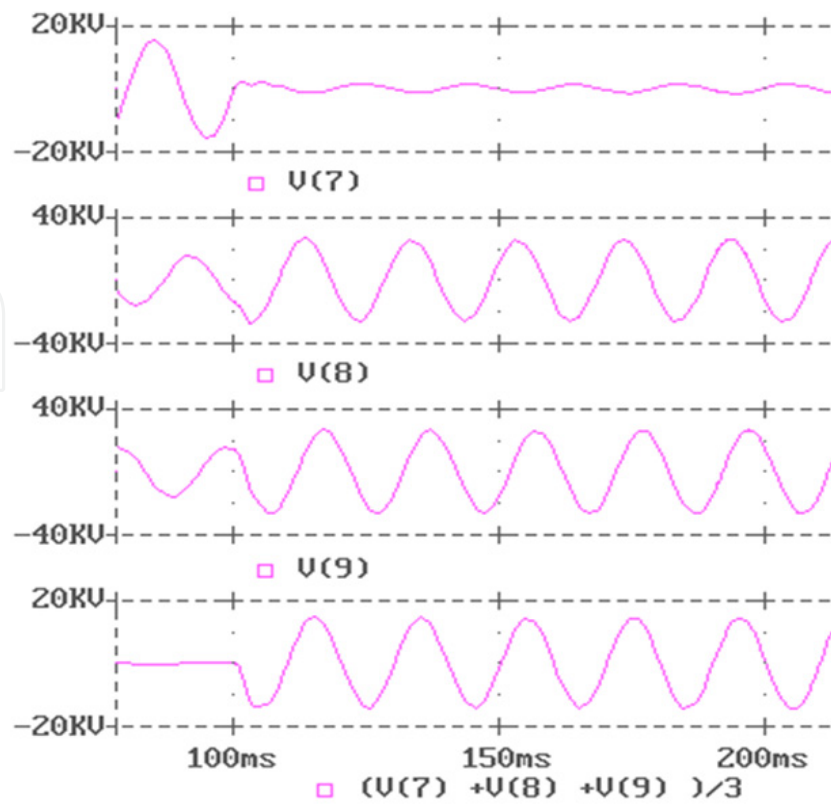
**Figure 22.** Time variation of the voltages when MVN is at resonance, $R_t = 1\Omega$, $\alpha = 0°$
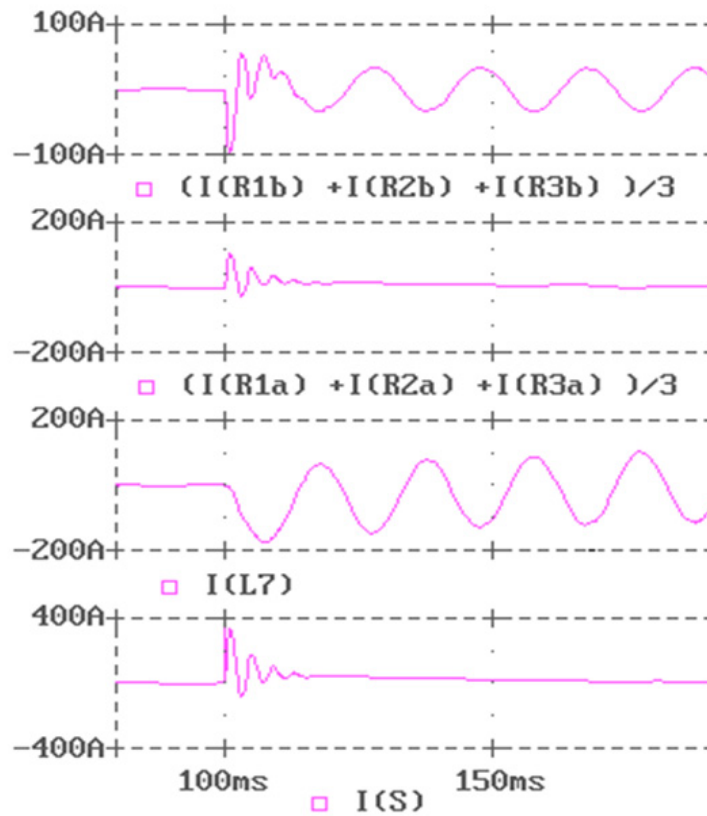
Figure 23. Time variation of the currents when MVN is at resonance , $R_t = 1\Omega$, $\alpha = 45°$
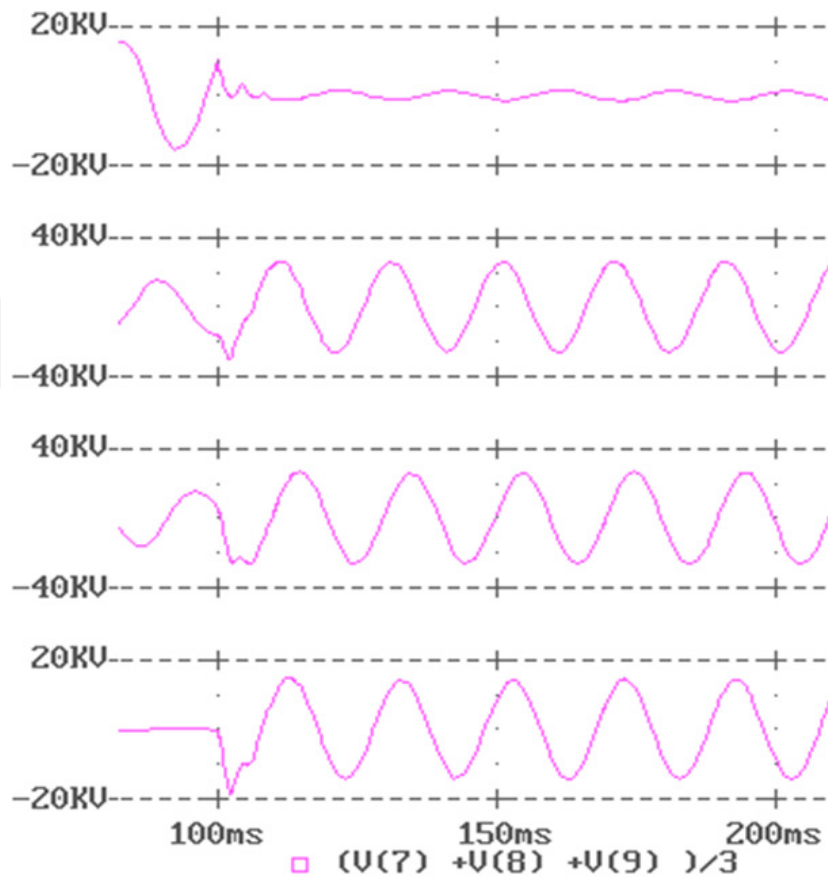
**Figure 24.** Time variation of the voltages when MVN is at resonance, $R_t = 1\Omega$, $\alpha = 45°$
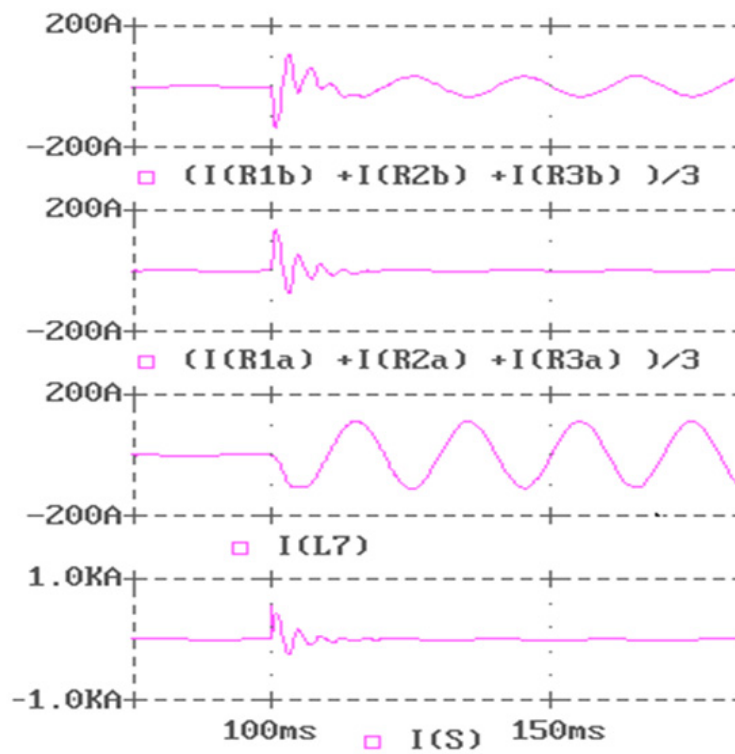
Figure 25. Time variation of the currents when MVN is at resonance , $R_t = 1\Omega$, $\alpha = 90°$
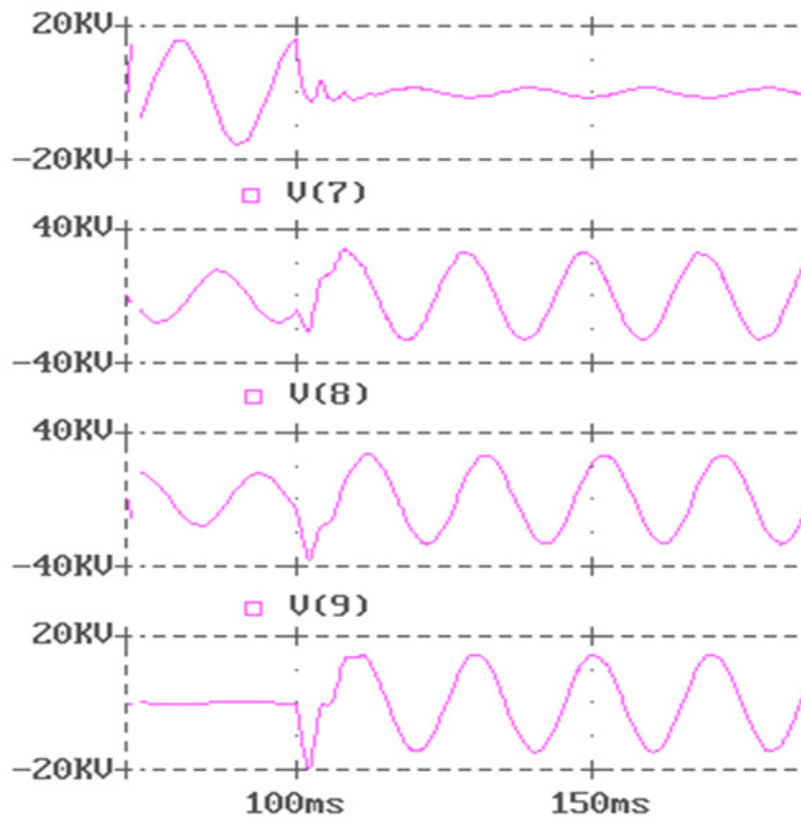
Figure 26. Time variation of the voltages when MVN is at resonance, $R_t = 1\Omega$, $\alpha = 90°$
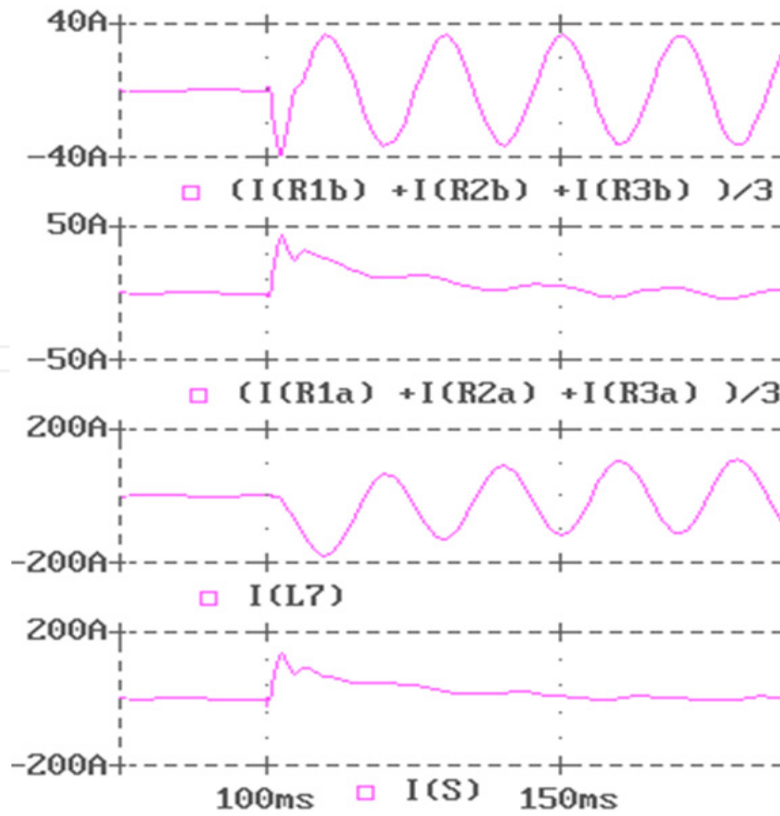
**Figure 27.** Time variation of the currents when MVN is at resonance , $R_t = 10\Omega$, $\alpha = 0°$
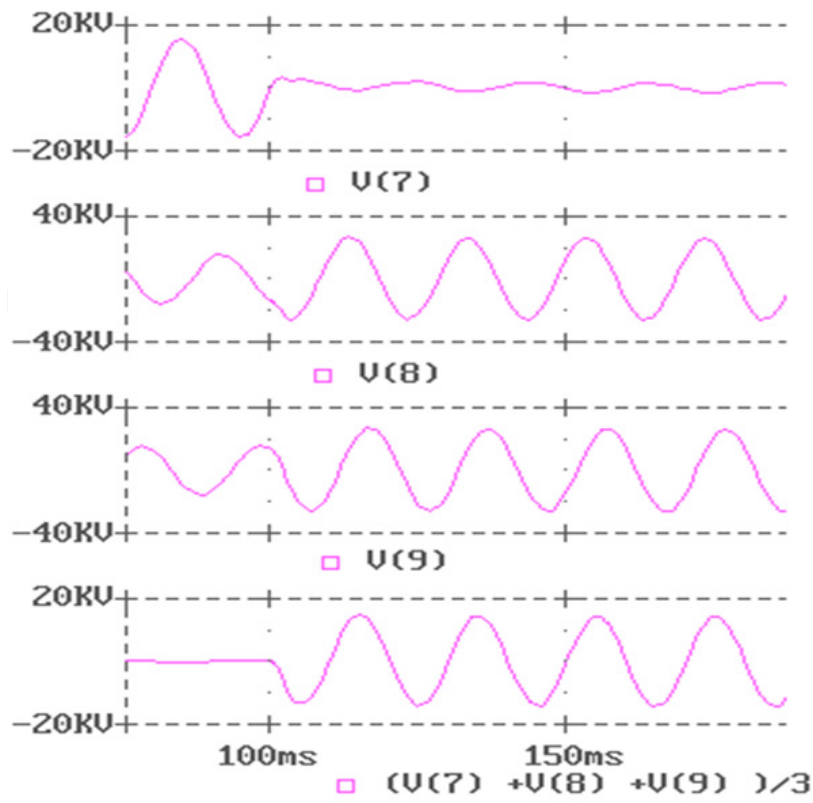
Figure 28. Time variation of the voltages when MVN is at resonance, $R_t = 10\Omega$, $\alpha = 0°$
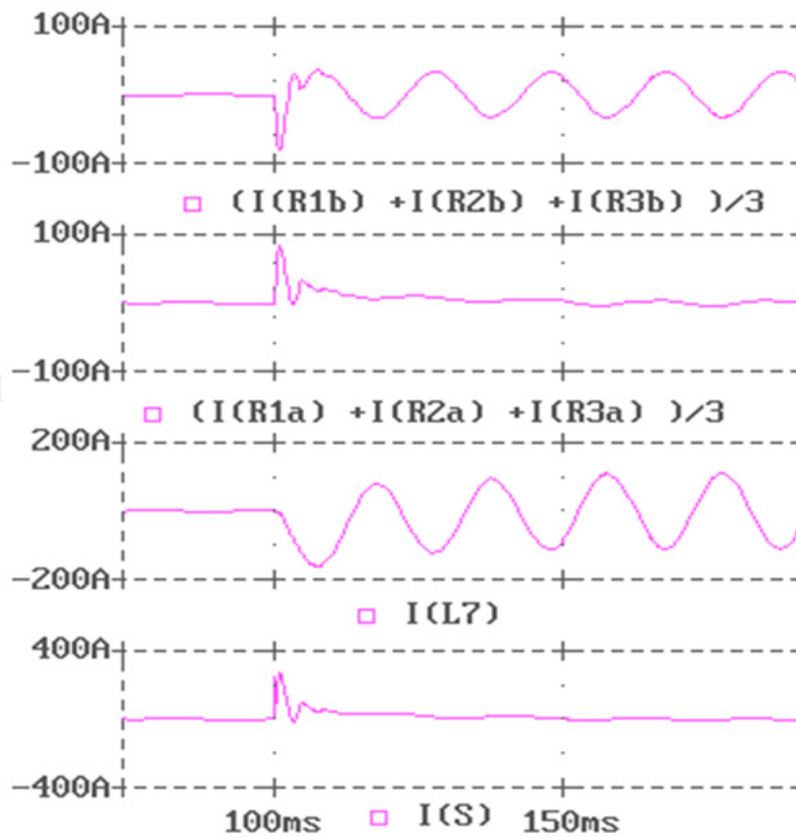
Figure 29. Time variation of the currents when MVN is at resonance , $R_t = 10\Omega$, $\alpha = 45°$
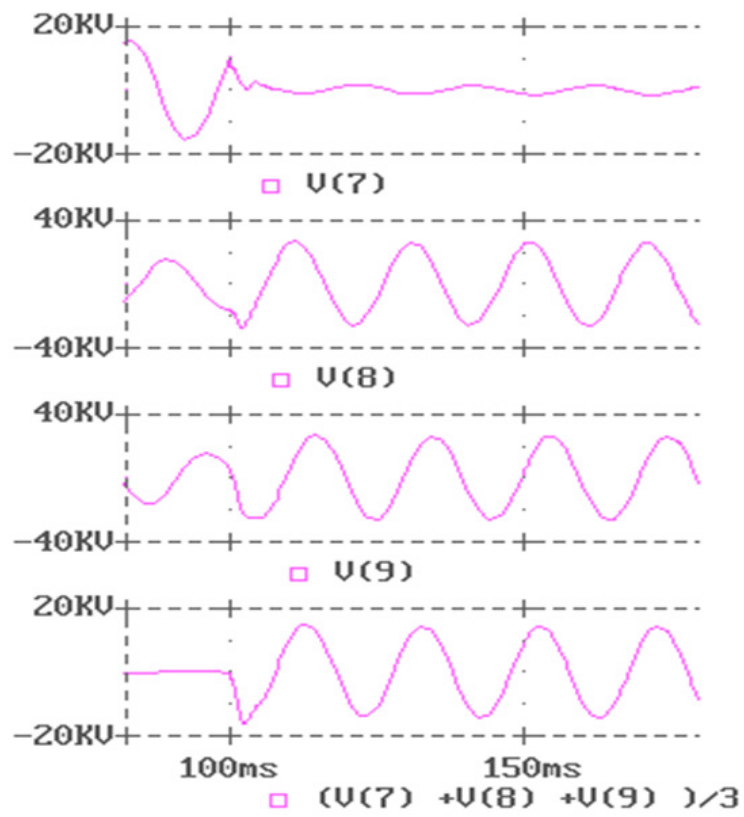
Figure 30. Time variation of the voltages when MVN is at resonance, Rt = 10Ω, α = 45°
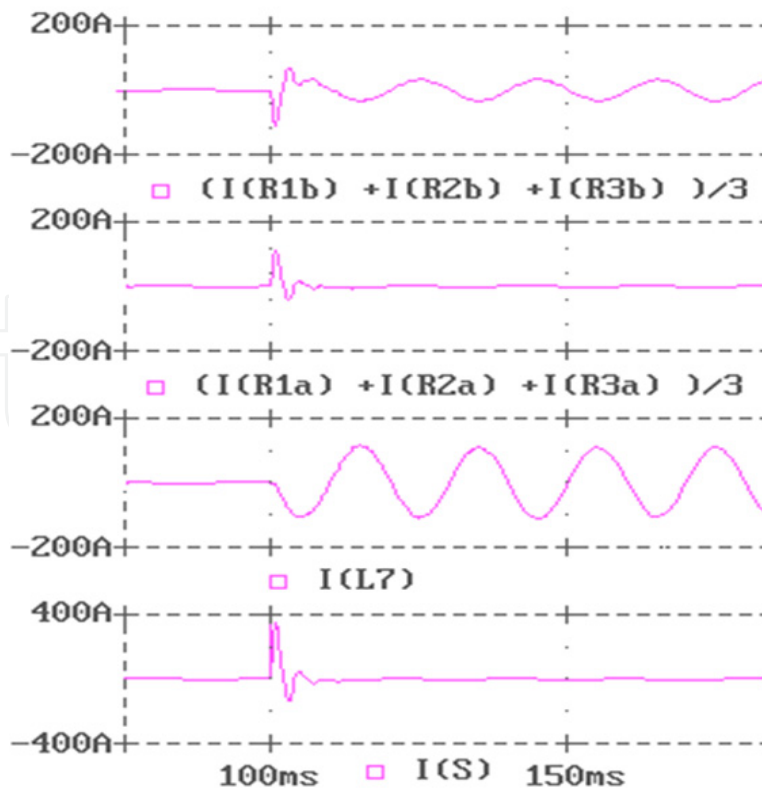
Figure 31. Time variation of the currents when MVN is at resonance , Rt = 10Ω, α = 90°
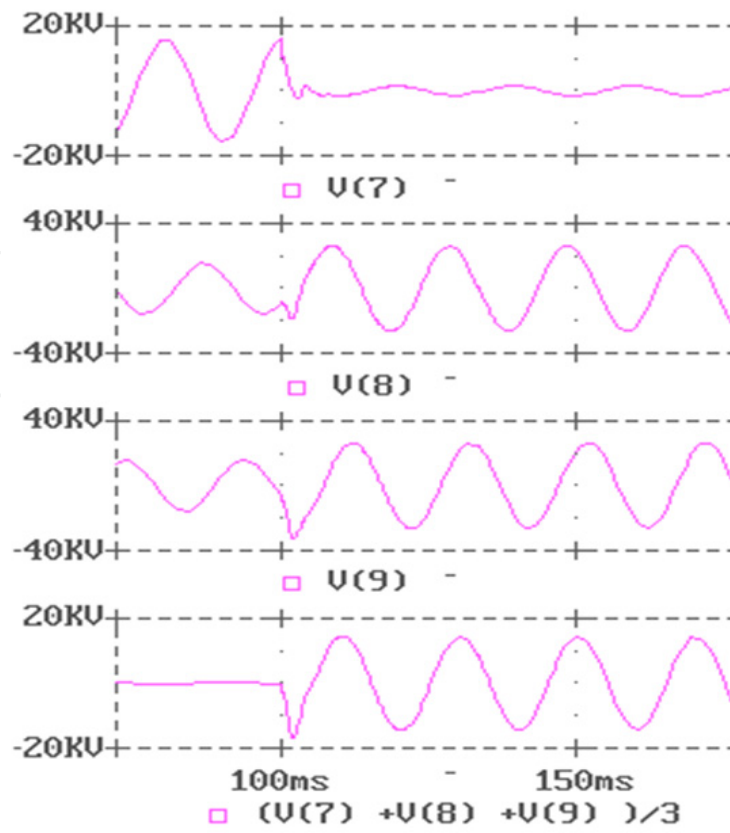
Figure 32. Time variation of the voltages when MVN is at resonance, $R_t = 10\Omega$, $\alpha = 90°$
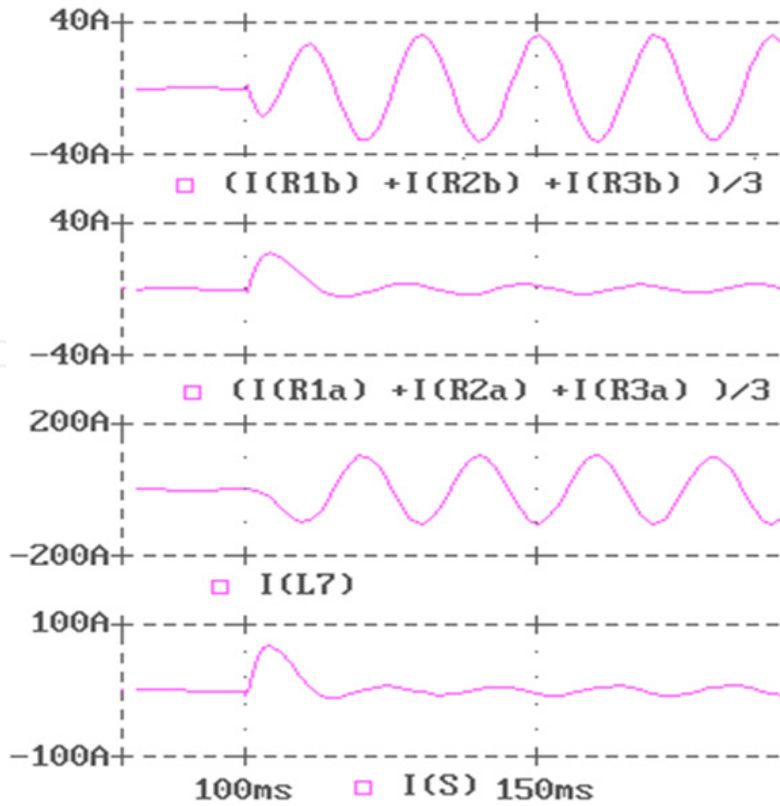
Figure 33. Time variation of the currents when MVN is at resonance , $R_t = 100\Omega$, $\alpha = 0°$
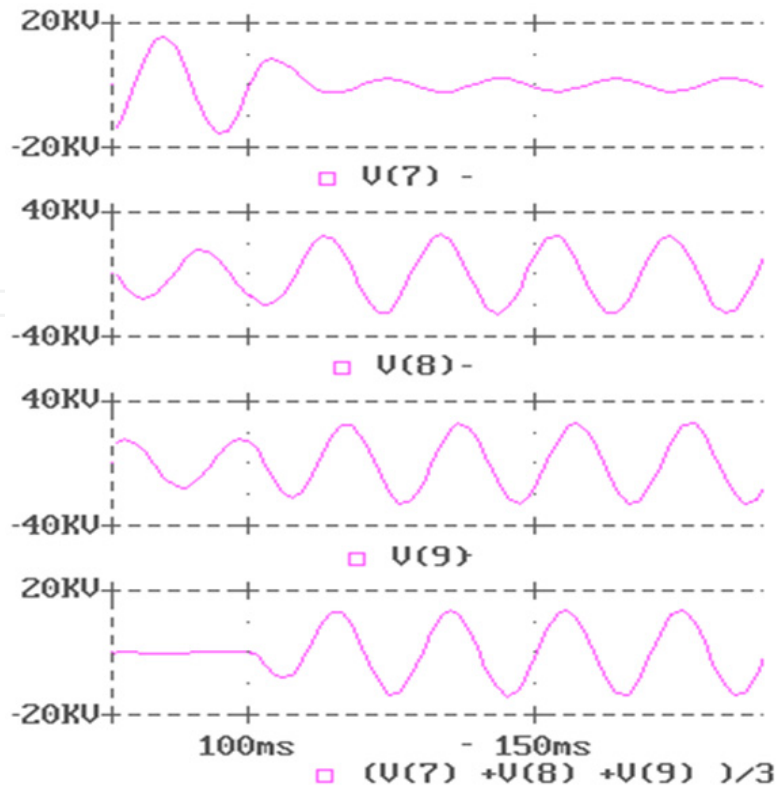
Figure 34. Time variation of the voltages when MVN is at resonance, $R_t = 100\Omega$, $\alpha = 0°$
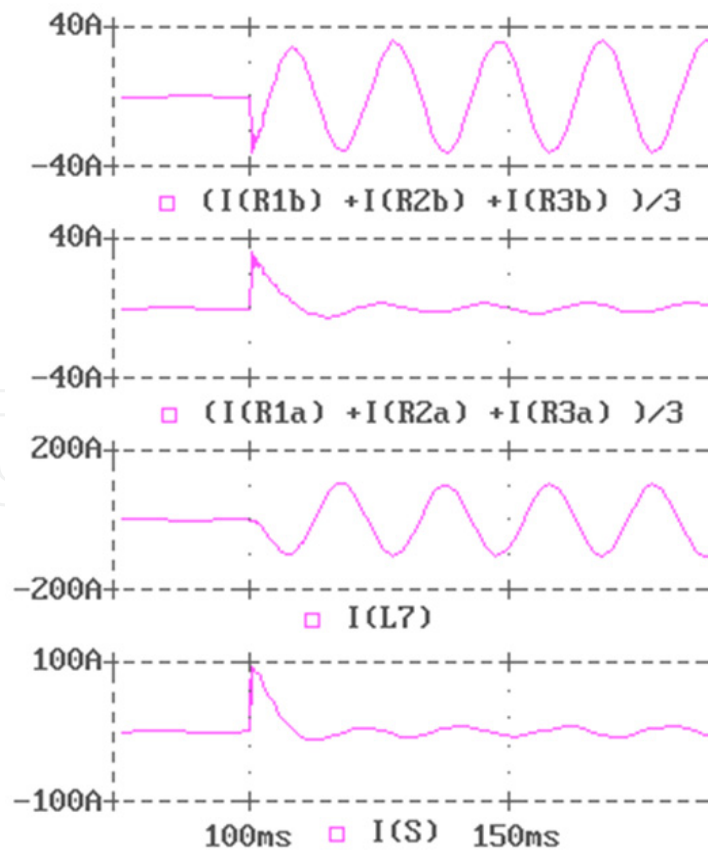
Figure 35. Time variation of the currents when MVN is at resonance , $R_t = 100\Omega$, $\alpha = 45°$
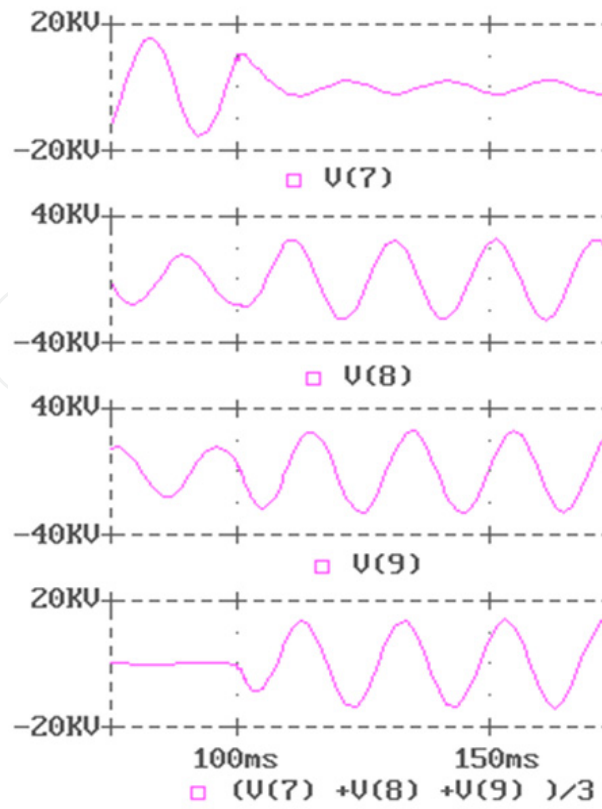
Figure 36. Time variation of the voltages when MVN is at resonance, $R_t = 100\Omega$, $\alpha = 45°$
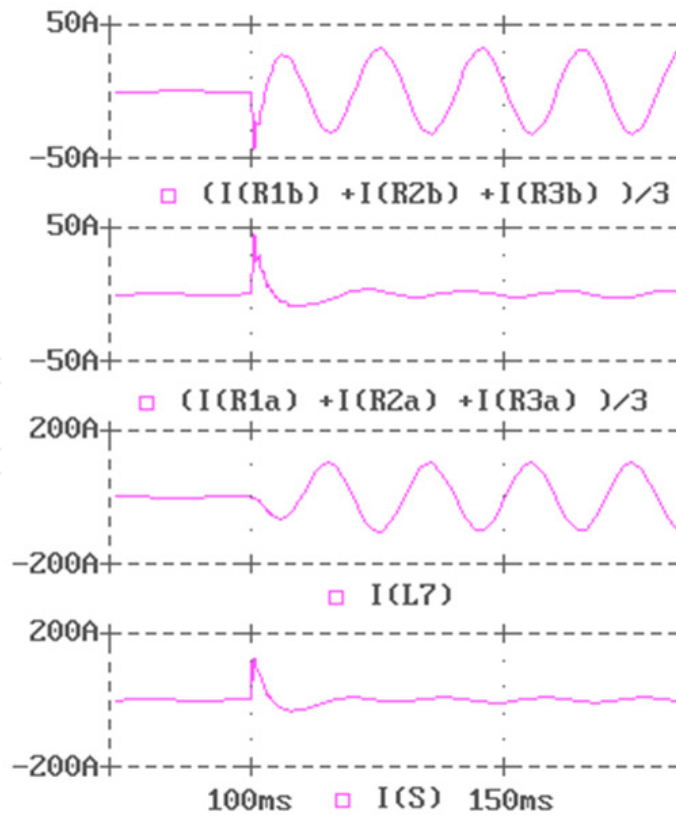

Figure 37. Time variation of the currents when MVN is at resonance , $R_t = 100\Omega$, $\alpha = 90°$
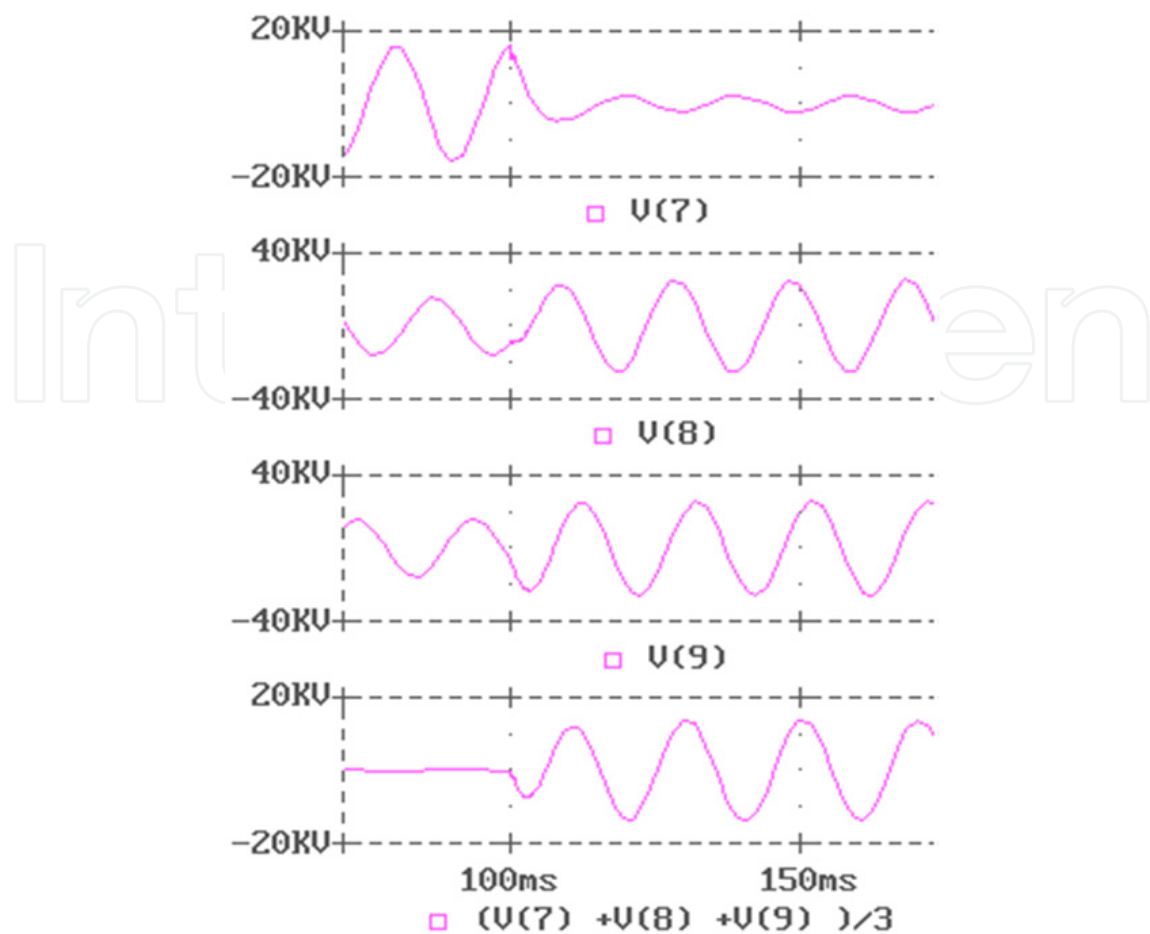
Figure 38. Time variation of the voltages when MVN is at resonance, $R_t = 100\Omega$, $\alpha = 90°$

4.2.2. The double phase-to-ground fault

The same simulation model from Fig. 8 is used with the switch VSa closed, and after 20ms the switch VSb is connected also. VSGOL remains in „closed" position.

The double phase to ground fault was simulated for neutral point grounded by compensation inductor and, respectively, by resistor.

In both cases R_t was considered consecutively with 1Ω, 100Ω, 1000Ω trough VSa switch and with 1Ω trough VSb .

In both cases $\alpha = 90°$ was considered, but also $\alpha = 0°$ was imposed for the situation with compensation inductor.

Also the situation with isolated neutral point was simulated, with same R_t values , but only with $\alpha = 90°$. (Curcanu et al., 2006).

The same symbols are used in oscillograms for the currents, just in addition the index "a" is used for the first faulty line (simulated by switch VSa) and the index "b" for the second faulty line (VSb). For the voltages the symbols are quite the same as those used previously.
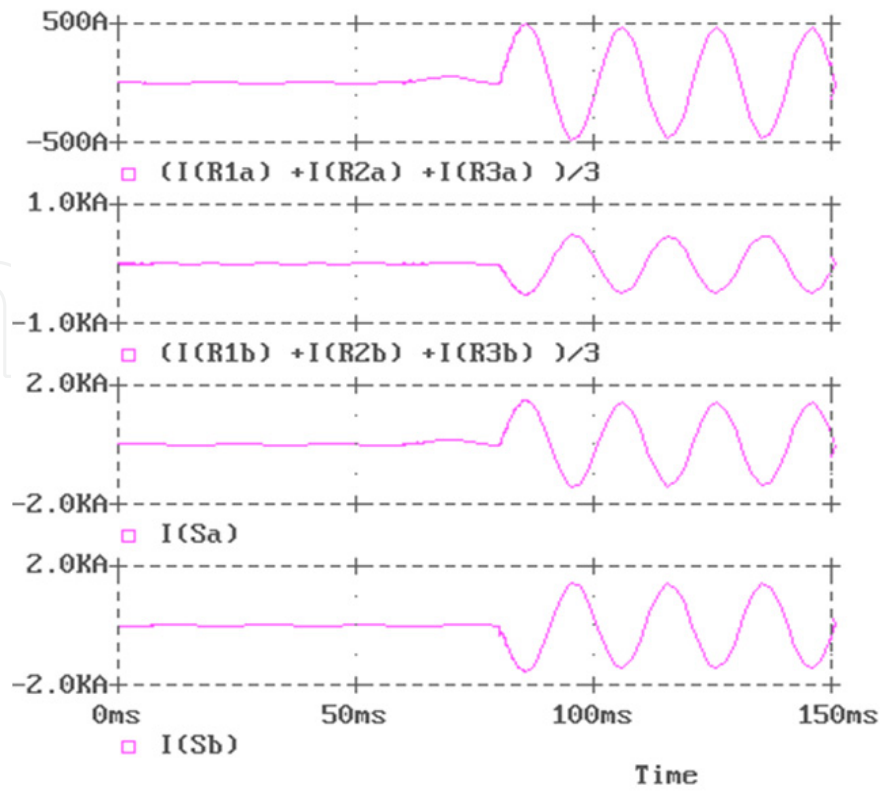
Figure 39. Time variation of the currents when MVN is at resonance , $R_t = 1\Omega$, $\alpha = 0°$
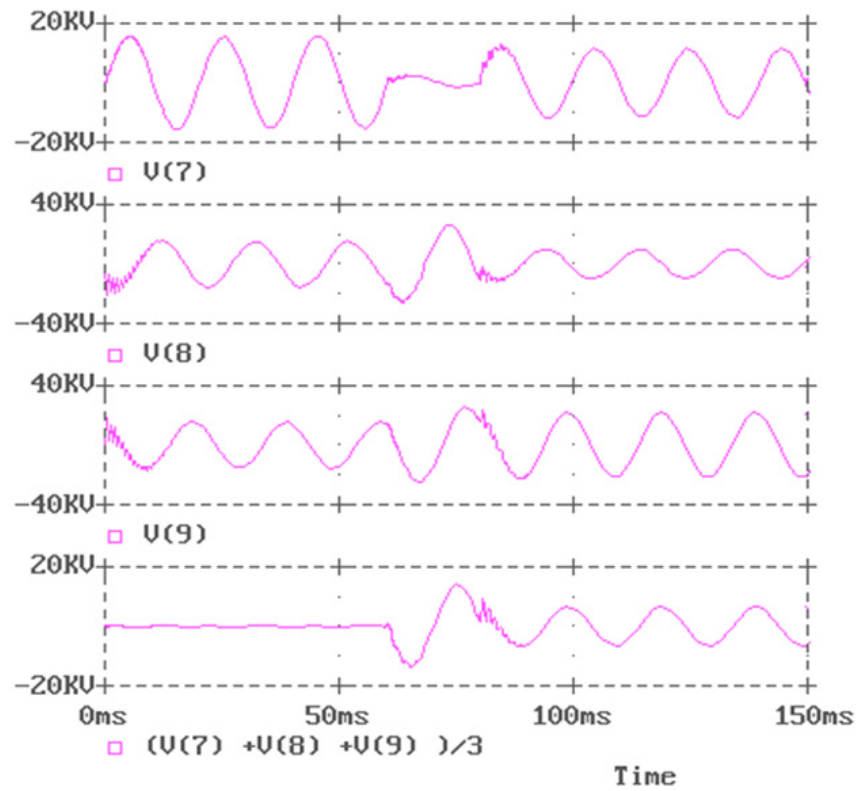

Figure 40. Time variation of the voltages when MVN is at resonance, $R_t = 1\Omega$, $\alpha = 0°$
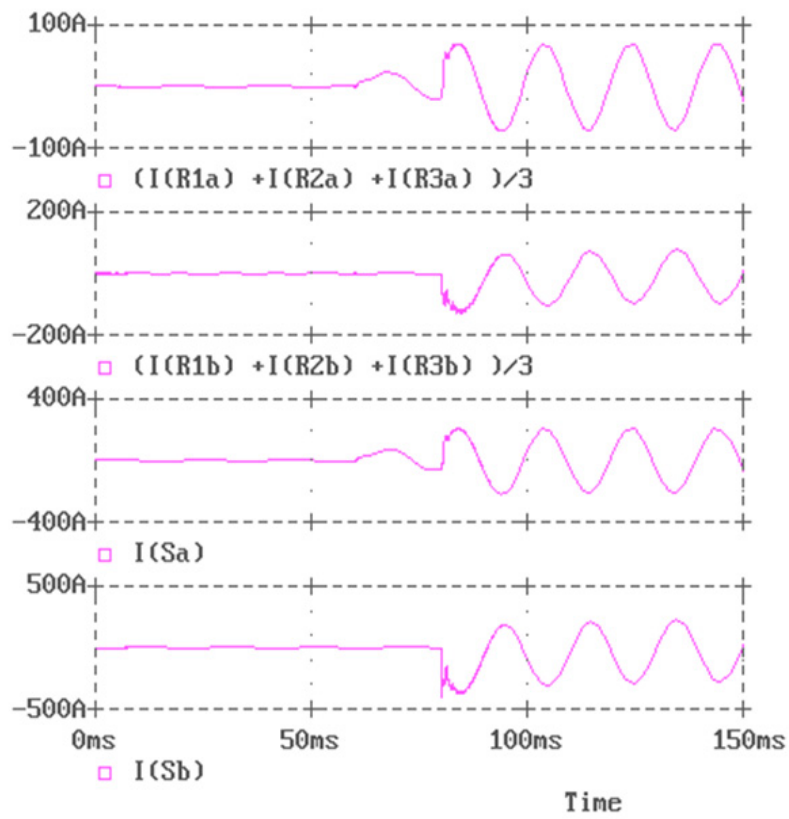
Figure 41. Time variation of the currents when MVN is at resonance , R$_t$ = 100Ω, α = 0°
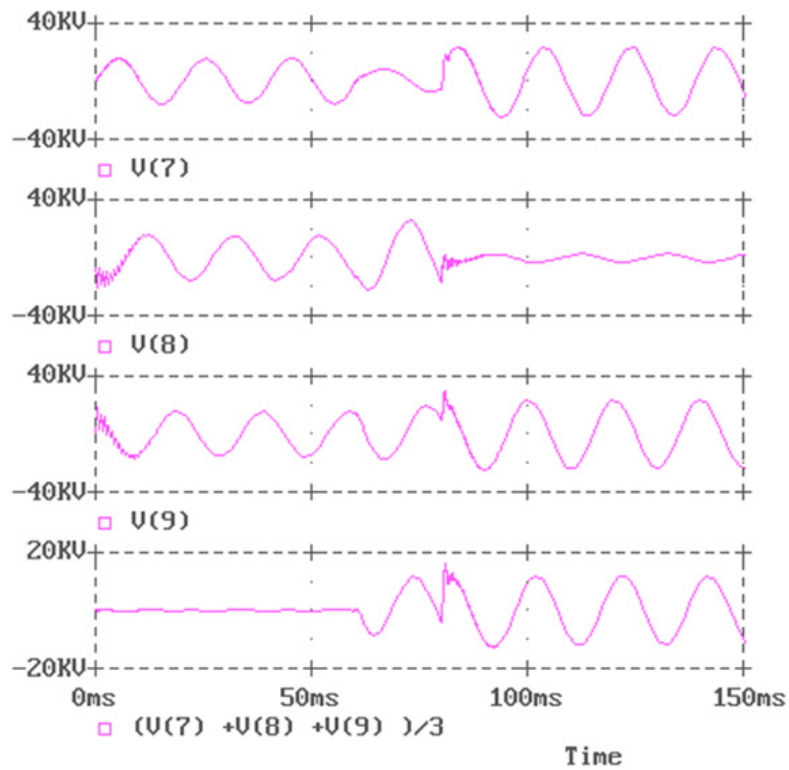
Figure 42. Time variation of the voltages when MVN is at resonance, R$_t$ = 100Ω, α = 0°
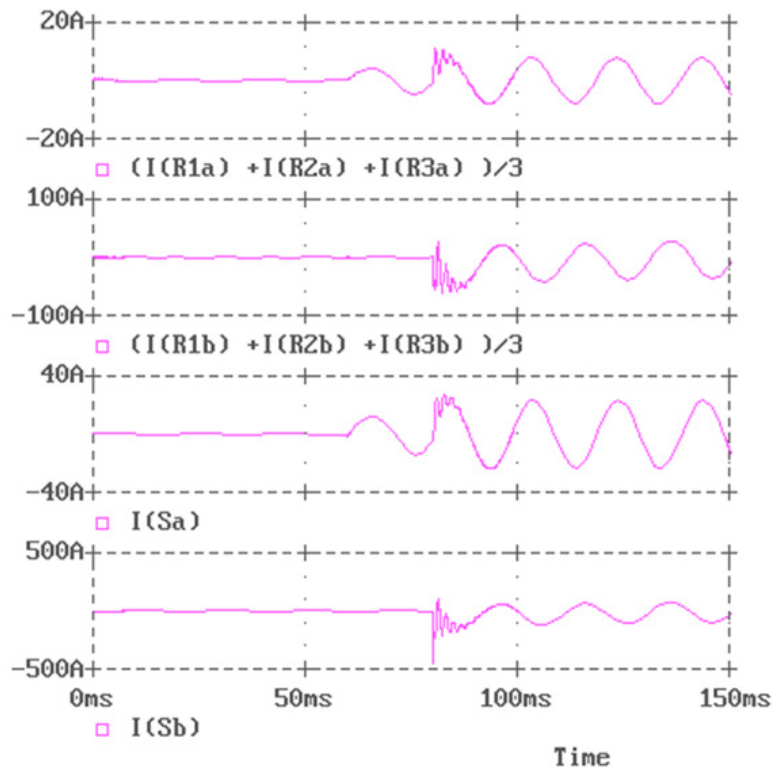
Figure 43. Time variation of the currents when MVN is at resonance , $R_t = 1000\Omega$, $\alpha = 0°$
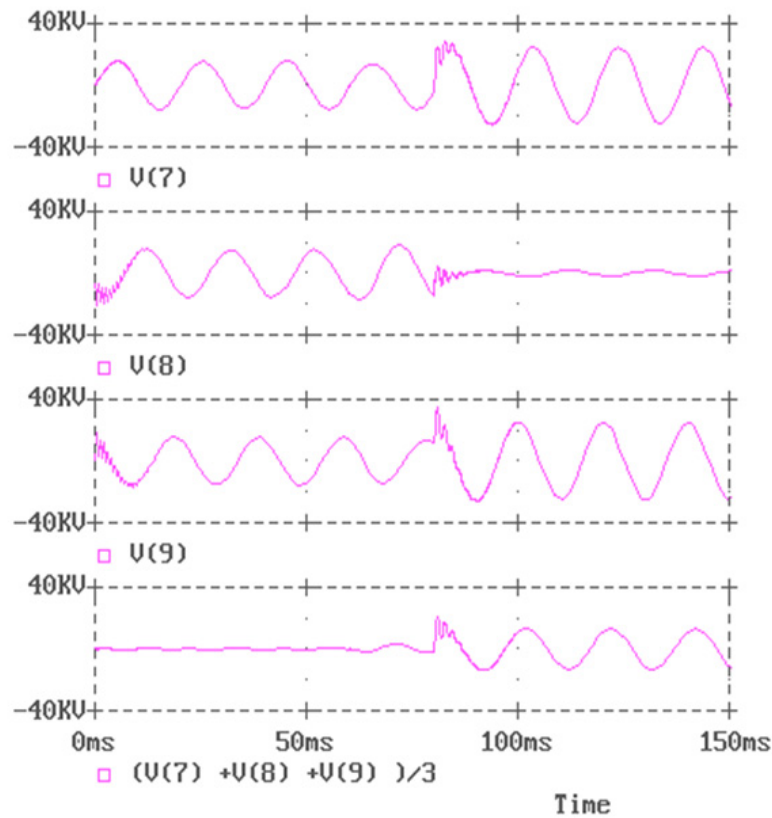
Figure 44. Time variation of the voltages when MVN is at resonance, $R_t = 1000\Omega$, $\alpha = 0°$
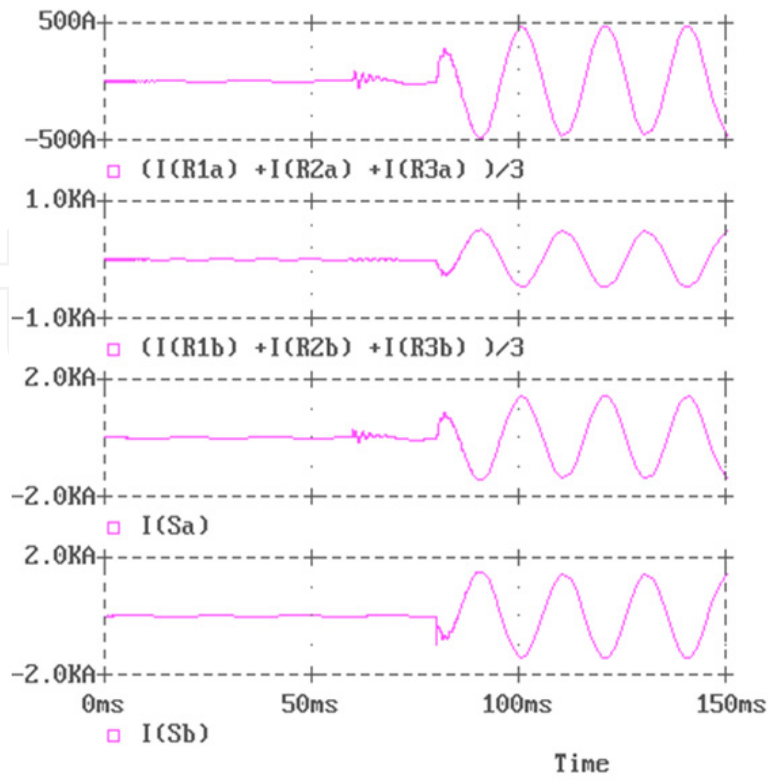
**Figure 45.** . Time variation of the currents when MVN is at resonance , $R_t = 1\Omega$, $\alpha = 90°$
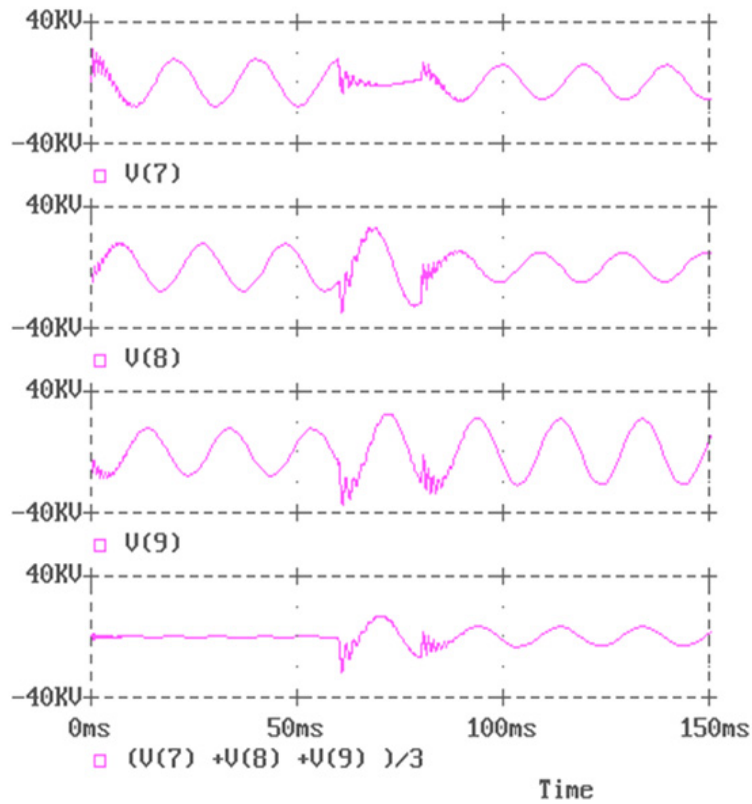
Figure 46. Time variation of the voltages when MVN is at resonance, $R_t = 1\Omega$, $\alpha = 90°$
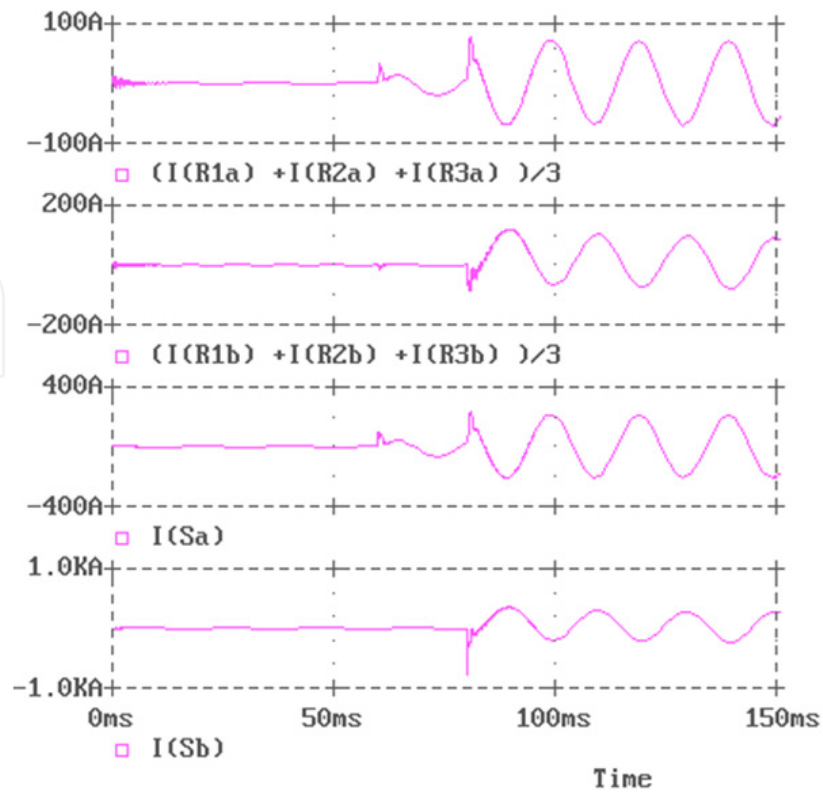
Figure 47. Time variation of the currents when MVN is at resonance , $R_t = 100\Omega$, $\alpha = 90°$
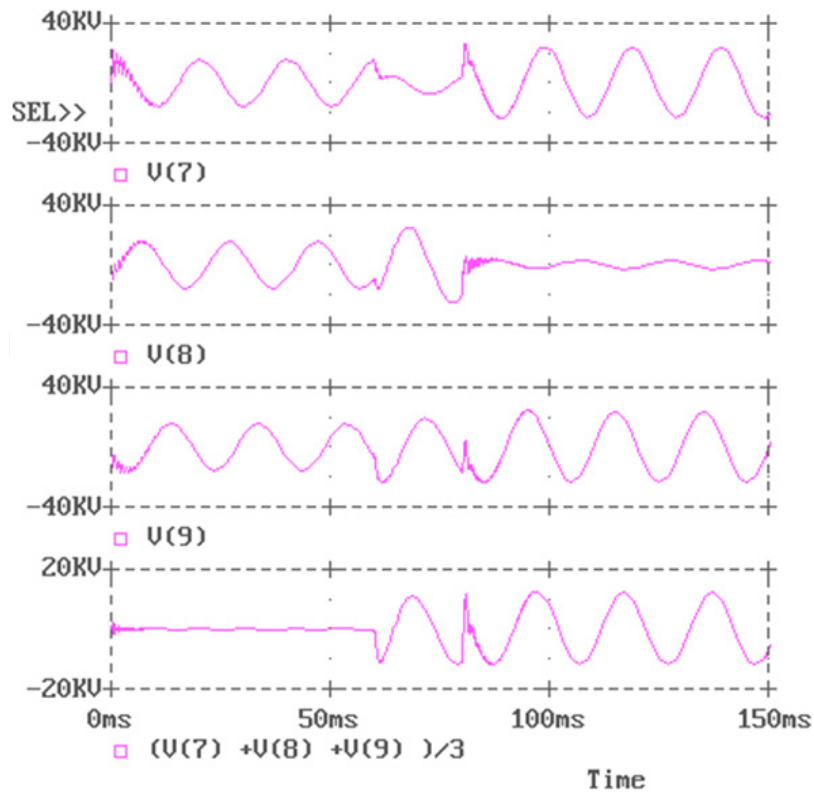
**Figure 48.** Time variation of the voltages when MVN is at resonance, $R_t = 100\Omega$, $\alpha = 90°$
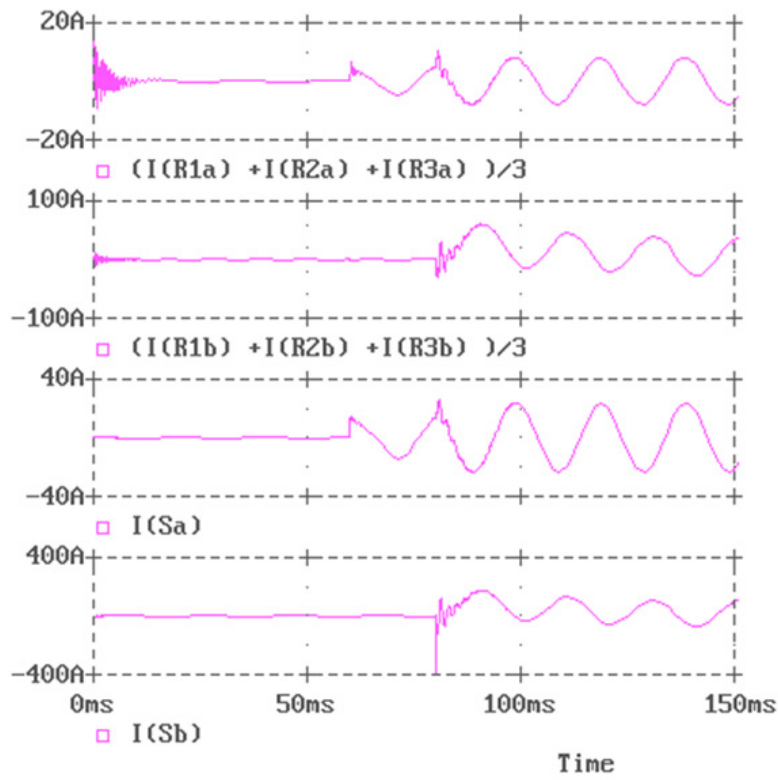
**Figure 49.** Time variation of the currents when MVN is at resonance , $R_t = 1000\Omega$, $\alpha = 90°$
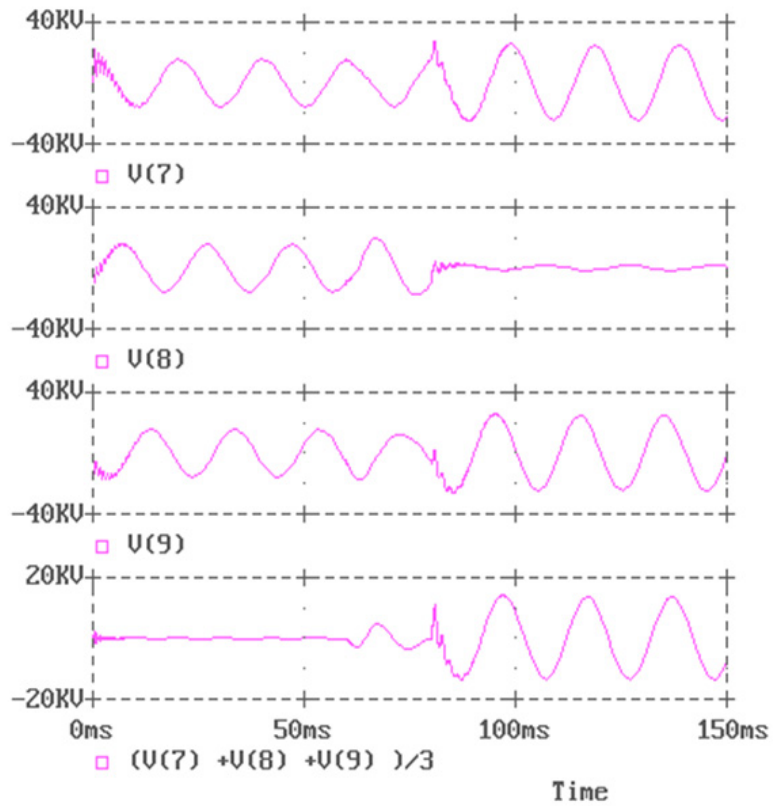
Figure 50. Time variation of the voltages when MVN is at resonance, $R_t = 1000\Omega$, $\alpha = 90°$

The double phase to ground fault has less important transient effects than the single phase to ground fault.

When the simple phase to ground fault occurs than the value of initial phase α is importans, but its variation is totaly insignifiant in the double phase to ground fault. The value of the resistance at the fault place is important in both fault types, the maximal value of the fault currents and the zero sequence currents depending strongly on the electric resistance at the fault place.

The oscillograms for the MVN grounded trough resistor are presented in Fig. 51 ... Fig. 54. The fault is simulated with the switch VSa and for $\alpha = 90°$ the transient is most important.

The current flowing trough the grounding resistor is calculated also and this is important because the value of this current is taken into account for the protection.

The resistance at the fault place is simulated with the switch VSa.
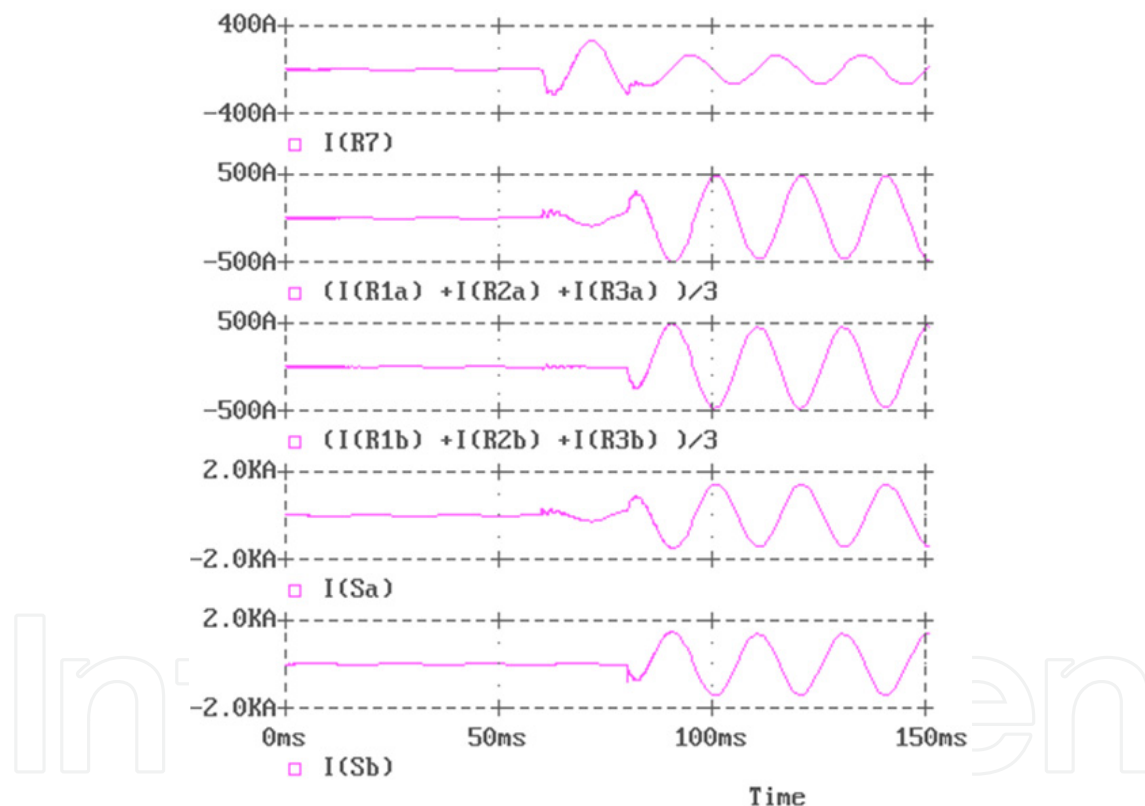
Figure 51. Time variation of the currents when MVN is grounded trough resistor, $R_t = 1\Omega$, $\alpha = 90°$

If the resistance at the fault place is increasing from 1Ω to 100Ω the current at the fault place is strongly decreasing from 1.8kA to 500A.

Oscillograms from Fig. 55 …Fig. 60 , for isolated neutral point of the MVN, show that the double phase to ground fault gives a heavier transient for voltages than for currents.

There is not an important difference between the transient produced by the double phase to ground fault in MVN with isolated neutral point compared with the MVN grounded trough

compensation inductor, but both cases are much heavier than the transient for MVN grounded trough resistor.
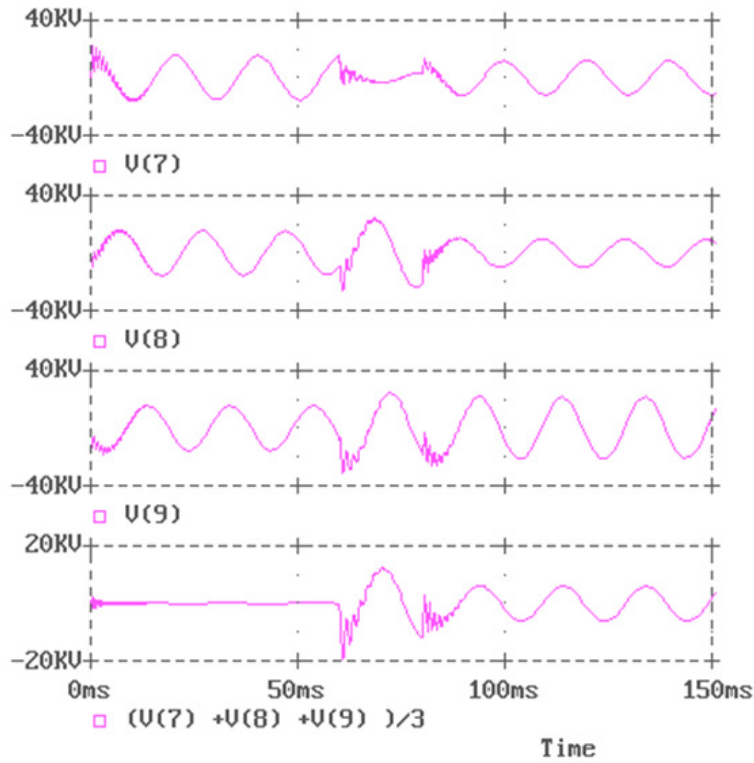
**Figure 52.** Time variation of the voltages when MVN is grounded trough resistor $R_t = 1\Omega$, $\alpha = 90°$
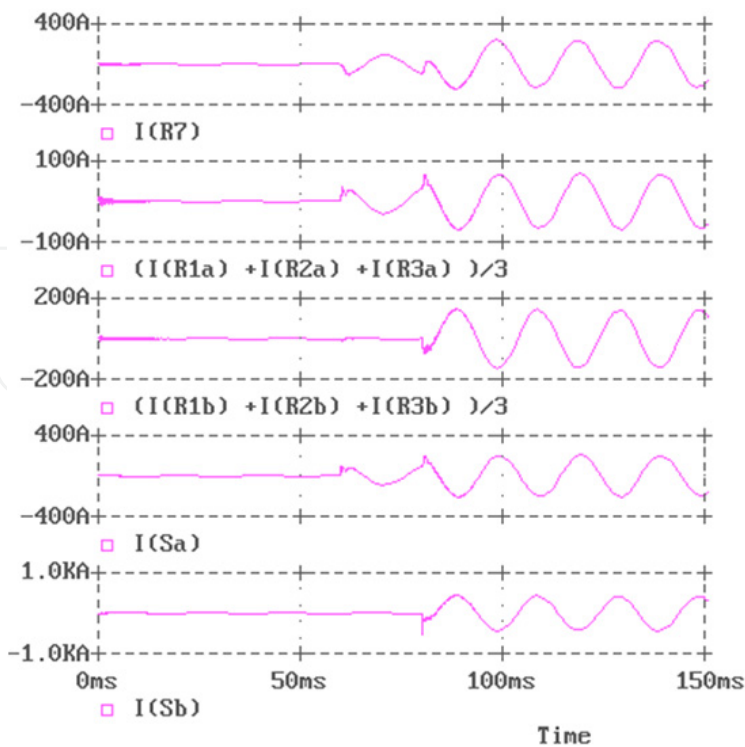
Figure 53. Time variation of the currents when MVN is grounded trough resistor, $R_t = 100\Omega$, $\alpha = 90°$
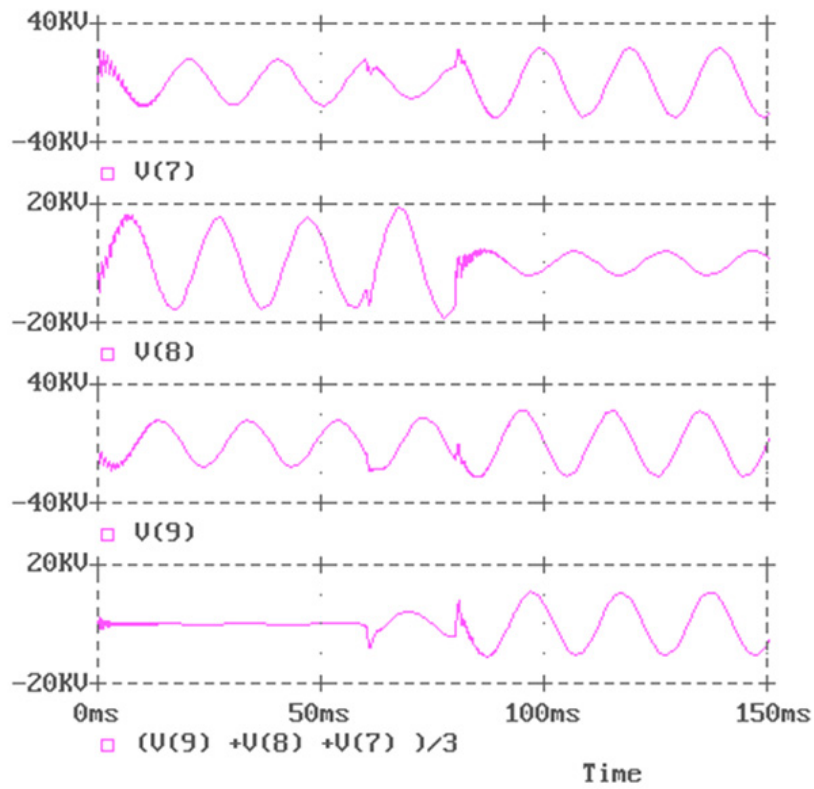
**Figure 54.** Time variation of the voltages when MVN is grounded trough resistor $R_t = 100\Omega$, $\alpha = 90°$
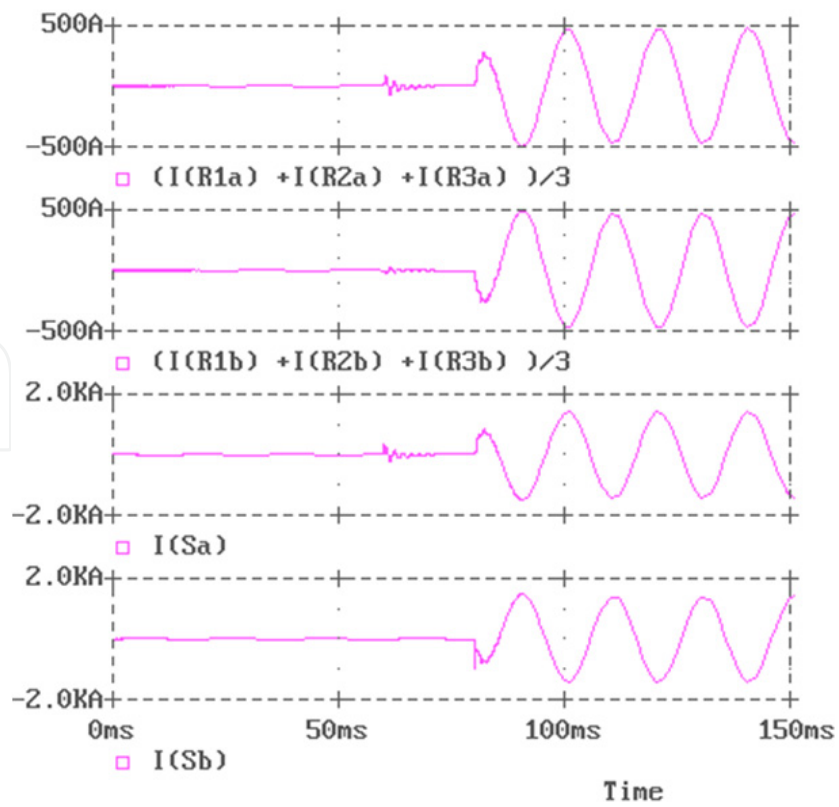
Figure 55. Time variation of the currents when the neutral point of MVN is isolated, $R_t = 1\Omega$, $\alpha = 90°$
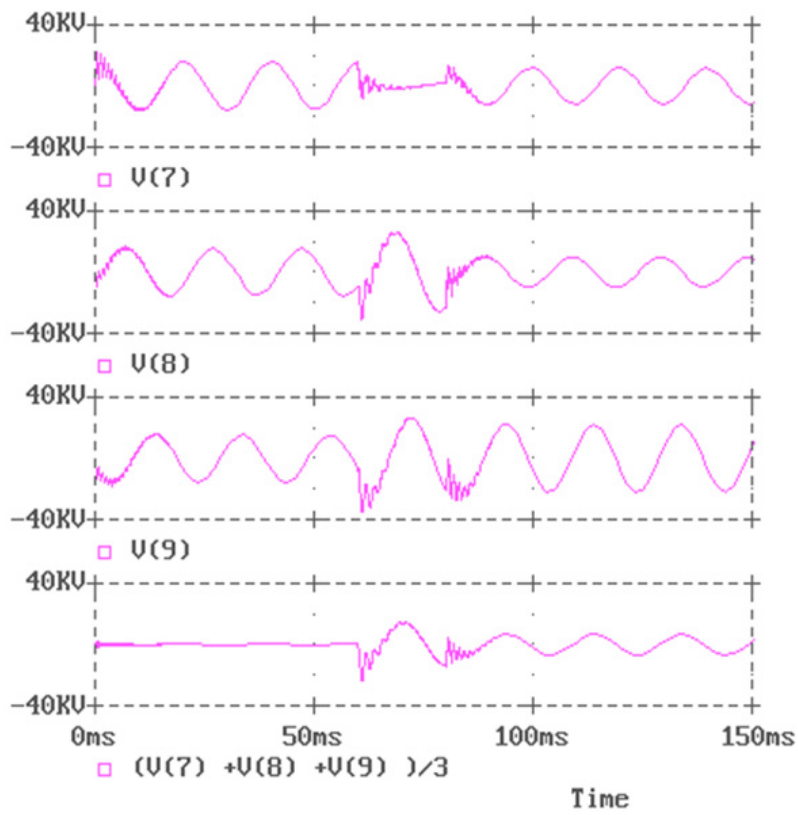
Figure 56. Time variation of the voltages when the neutral point of MVN is isolated, $R_t = 1\Omega$, $\alpha = 90°$
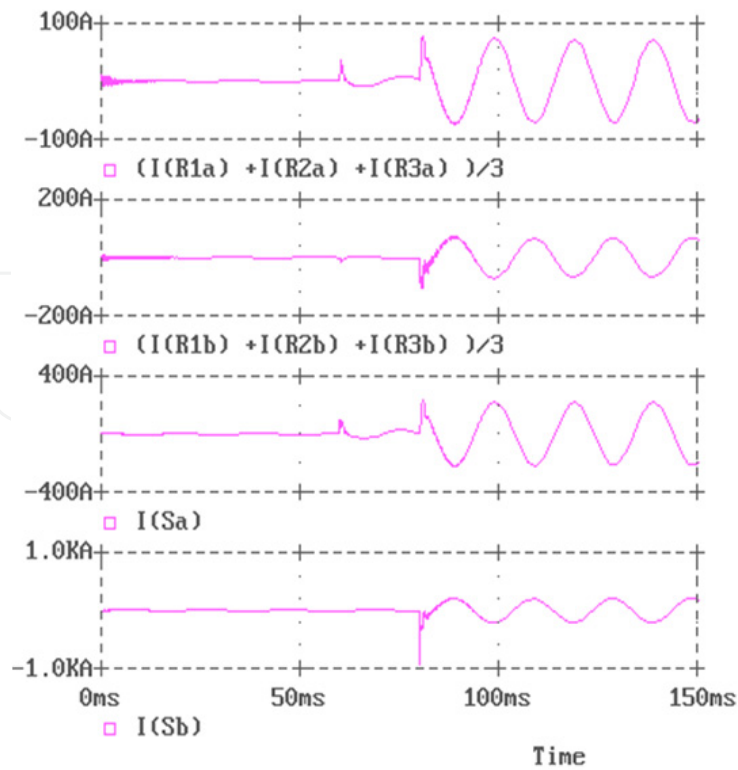
Figure 57. Time variation of the currents when the neutral point of MVN is isolated, $R_t = 100\Omega$, $\alpha = 90°$
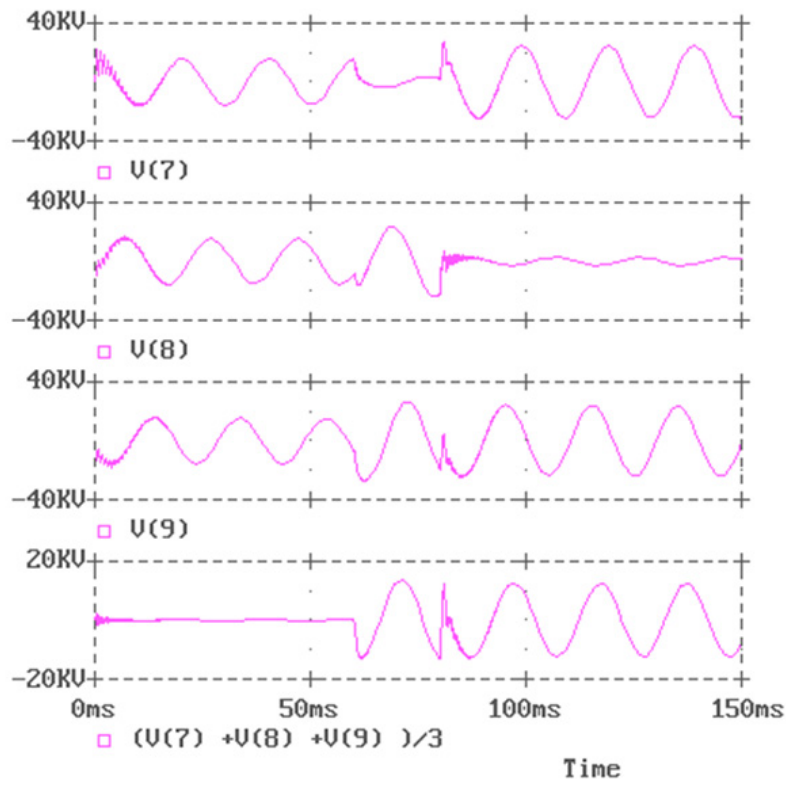
Figure 58. Time variation of the voltages when the neutral point of MVN is isolated, $R_t = 100\Omega$, $\alpha = 90°$
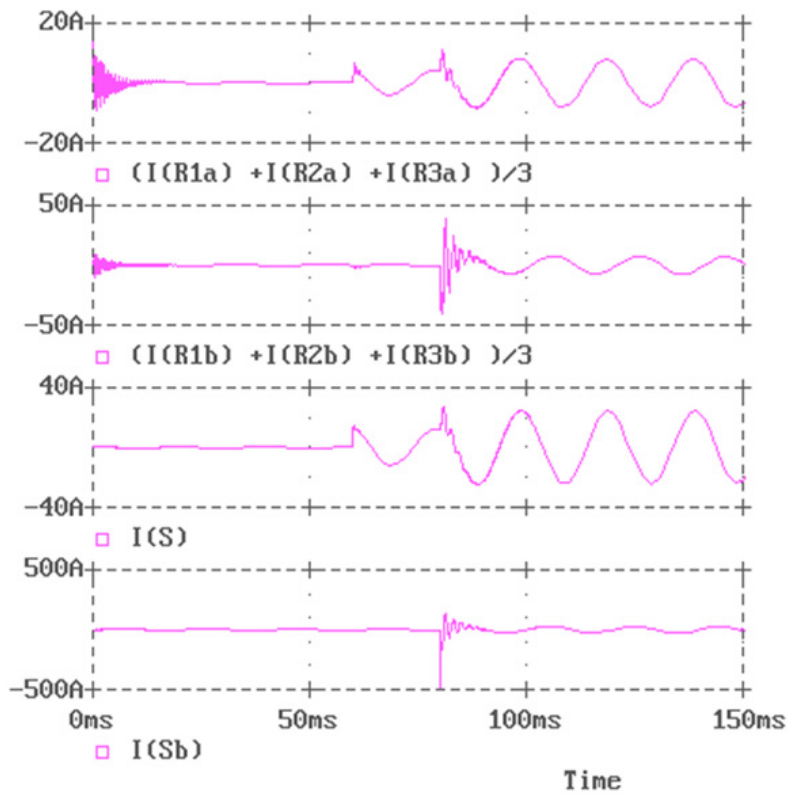

Figure 59. Time variation of the currents when the neutral point of MVN is isolated, $R_t = 1000\Omega$, $\alpha = 90°$
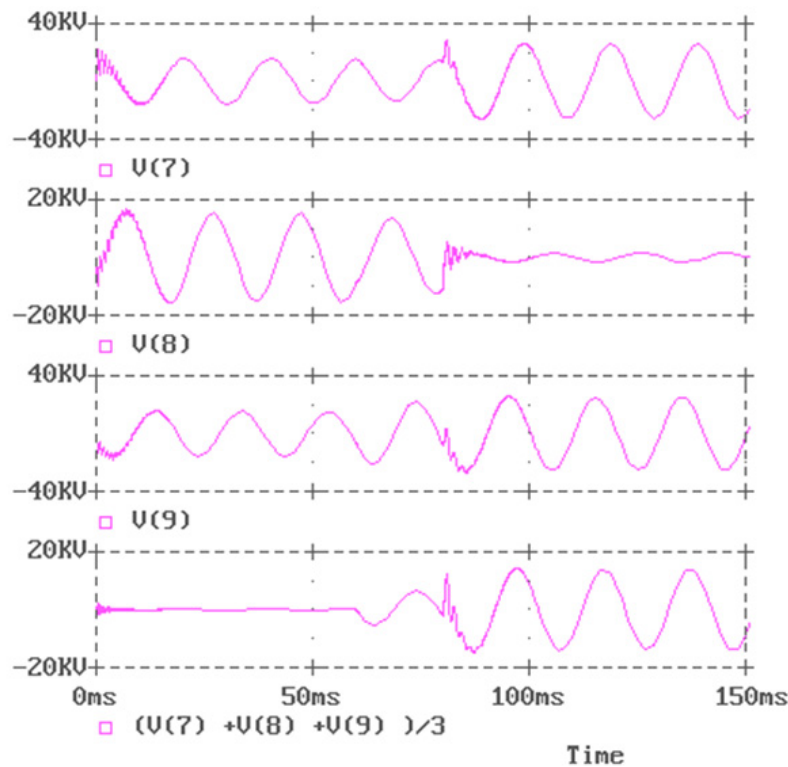
Figure 60. Time variation of the voltages when the neutral point of MVN is isolated, $R_t = 1000\Omega$, $\alpha = 90°$

The greater values of the currents at the two fault places, when the double phase to ground fault is produced, give high thermic solicitation to the instalation, as well as, higher values of the step voltages. This situatiom is dangerous for human being and animals, especially if this events are situated near the earth plate.

The time variation at the two fault places is far from being the same, no matter what grounding methos is used for the neutral point of the MVN.

4.2.3. The interrupted conductor with ground contact towards the customer fault

For this simulation VSGOL is opened , as if the phase conductor would be interrupted, and with a 20ms delay VSa is connected (simulating the ground contact of the broken conductor). The switch VSb remains opened.

The MVN functioning at resonance, with compensation inductor, was simulated with three values of R_t, namely 1Ω, 10Ω, 100Ω. Two values for α were taken into account, $0°$, respectively $90°$.

The equivalent capacitance of the phase conductor from the fault to the consumers is simulated by:

- C_{101a} is simulating the capacitance of phase 1 from the fault place to the bars of the MV transformer station
- C_{102a} represents the model for the capacitance of the phase conductor from the fault place to the consumers supplied by the faulty line.

Two possible situations are considered: $C_{101a} = C_{102a}$, and $C_{102a} = 0,1C_{101a}$.
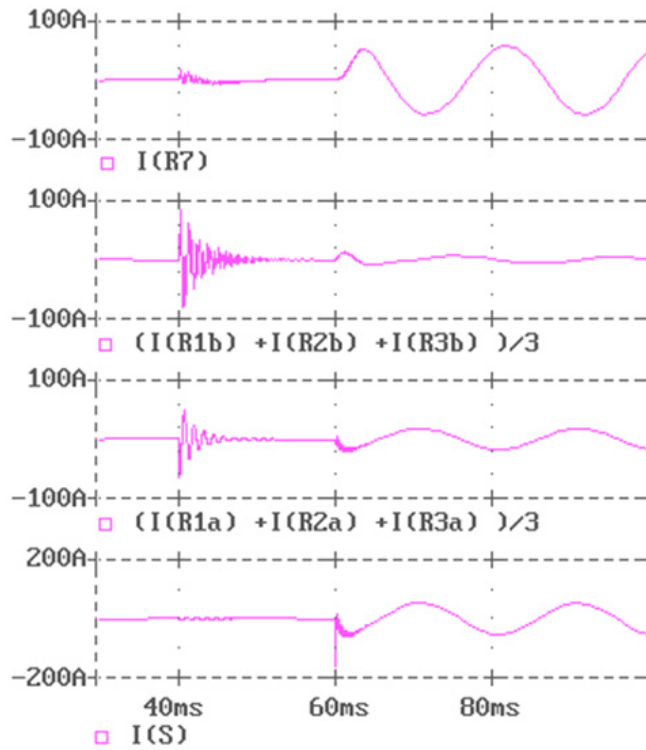
Figure 61. Time variation of the currents, neutral point of MVN is grounded by resistor and $R_t = 1\Omega$, $\alpha = 90°$, $C_{101a} = 9C_{102a}$
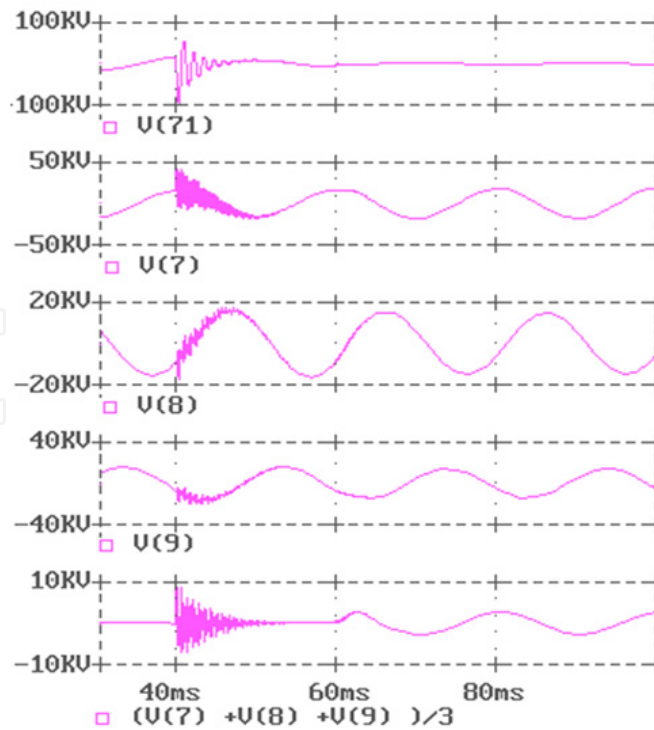
Figure 62. Time variation of the voltages, neutral point of MVN is grounded by resistor and $R_t = 1\Omega$, $\alpha = 90°$, $C_{101a} = 9C_{102a}$
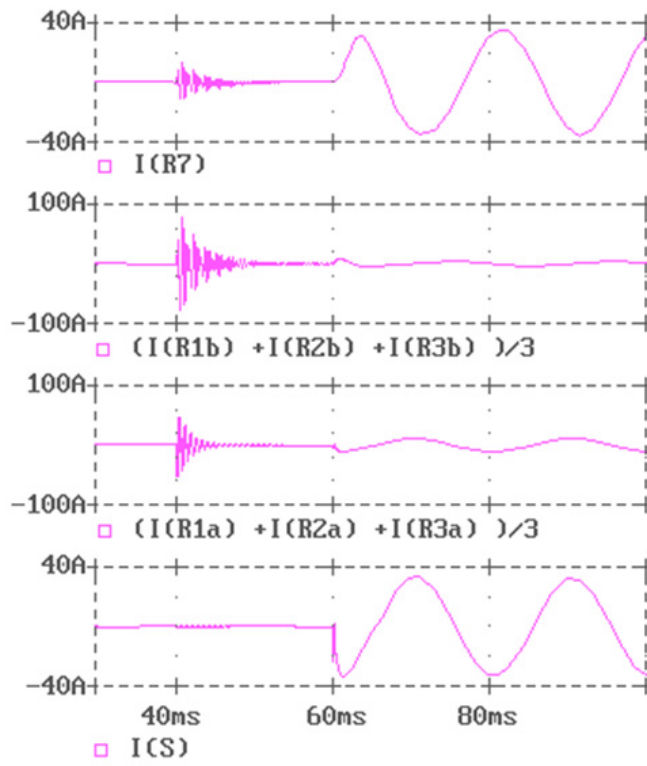
Figure 63. Time variation of the currents, neutral point of MVN is grounded by resistor and $R_t = 100\Omega$, $\alpha = 90°$, $C_{101a} = 9C_{102a}$
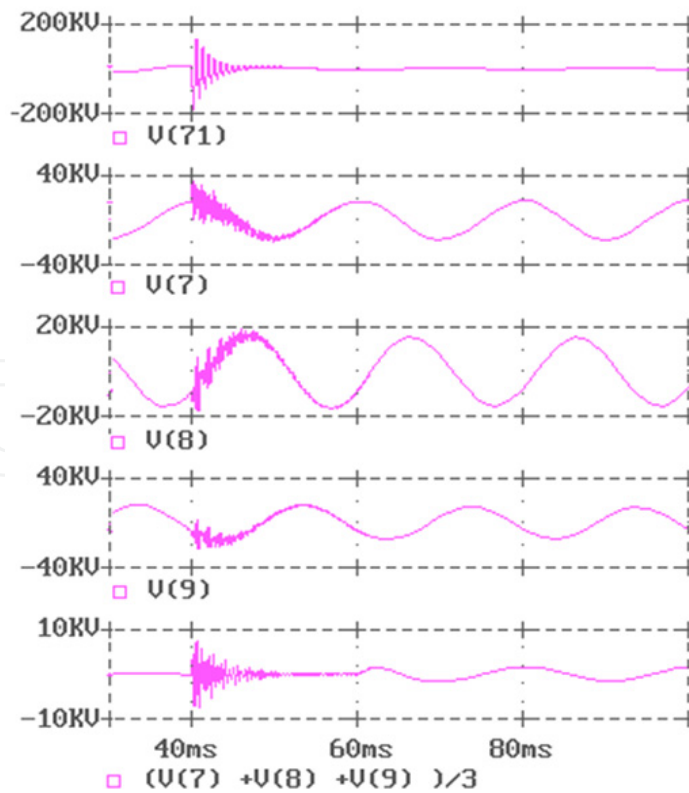

Figure 64. Time variation of the voltages, neutral point of MVN is grounded by resistor and $R_t = 100\Omega$, $\alpha = 90°$, $C_{101a} = 9C_{102a}$

In the oscillograms of the currents I(S) is the current to ground at the place of the fault, $I(R_7)$ is the current flowing trough the grounding resistor and the zero sequence current of the faulty line is $(I(R_{1a}) + I(R_{2a}) + I(R_{3a}))/3$. In the oscillogramms $(I(R_{1b}) + I(R_{2b}) + I(R_{3b}))/3$ is the zero sequence current of the healty "b" line.

The phase voltages are V(7), V(8), V(9), the zero sequence voltage on the bars of the MV transform station is (V(7) + V(8) + V(9))/3 and V(71) is the voltage of the broken conductor behind the fault place.

In each situation, either the grounding resistance is 1Ω, or 100Ω, the transient regime is stronger in the very moment of broking the phase conductor (t = 40 ms) than in the moment when the broken conductor contacts the ground (t = 60 ms). The voltage on the broken conductor might reach very high, dangerous values, jeopardizing the insulation of the line as well as the insulation of the consumer.

In Figs. 65 to 78 the oscillograms correspond to the MVN at resonance, with compensation inductor for grounding the neutral point. In this cases the current trough the compensation inductor is not represented because the protections used in MVN do not survey this current.

By the point of view of the overvoltages that might appear when the conductor is broken are more dangerous than the overvoltages in the case when the broken conductor is in contact with the ground.
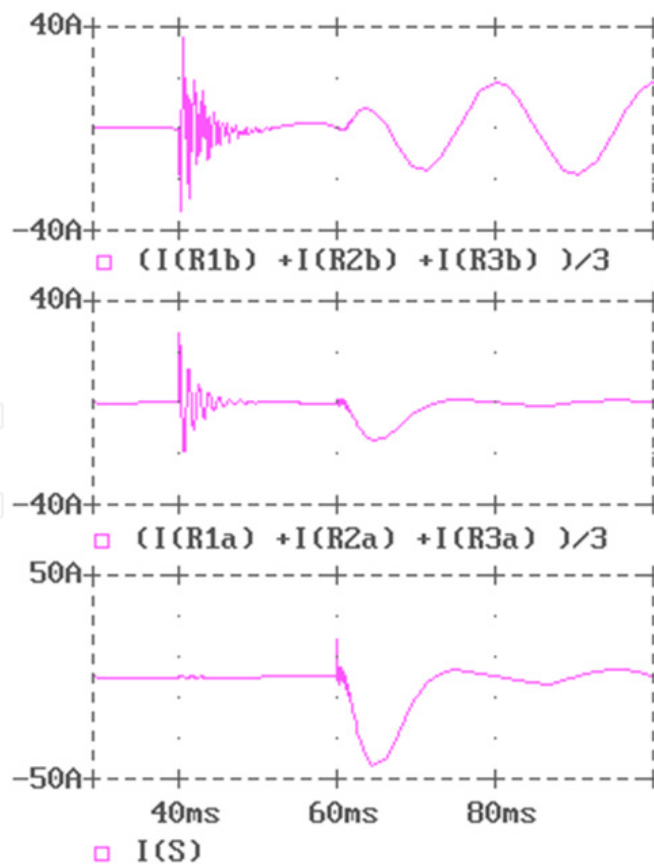
Figure 65. Time variation of the currents when MVN is at resonance, $R_t = 1\Omega$, $\alpha = 0°$, $C_{101a} = C_{102a}$
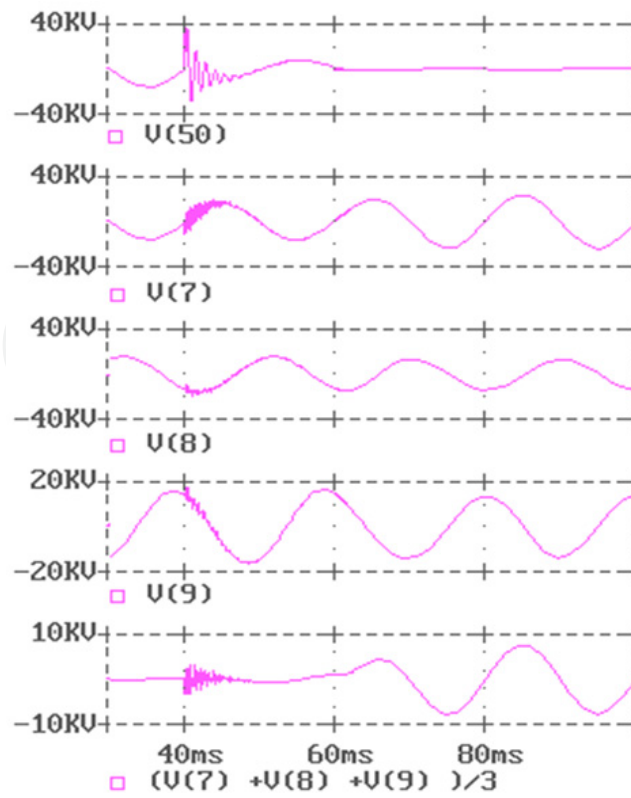
Figure 66. Time variation of the voltages, when MVN is at resonance, $R_t = 1\Omega$, $\alpha = 0°$, $C_{101a} = C_{102a}$
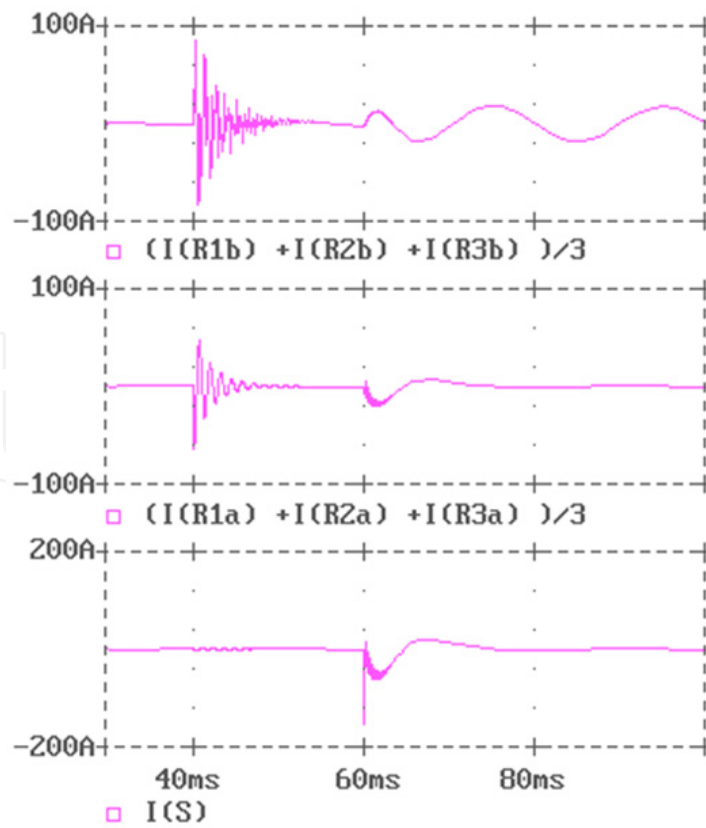
Figure 67. Time variation of the currents when MVN is at resonance, $R_t = 1\Omega$, $\alpha = 90°$, $C_{101a} = C_{102a}$
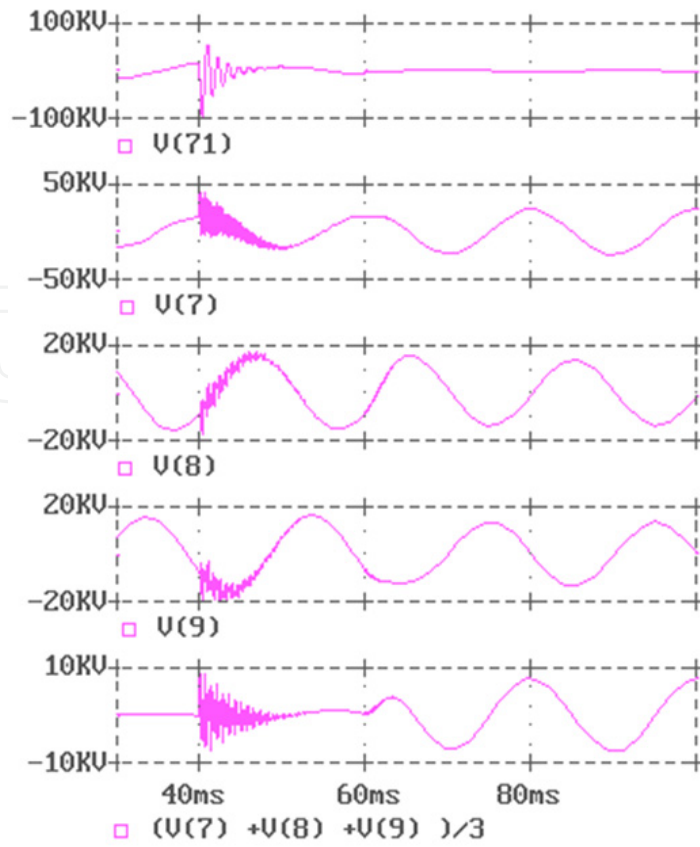
Figure 68. Time variation of the voltages, when MVN is at resonance, $R_t = 1\Omega$, $\alpha = 90°$, $C_{101a} = C_{102a}$
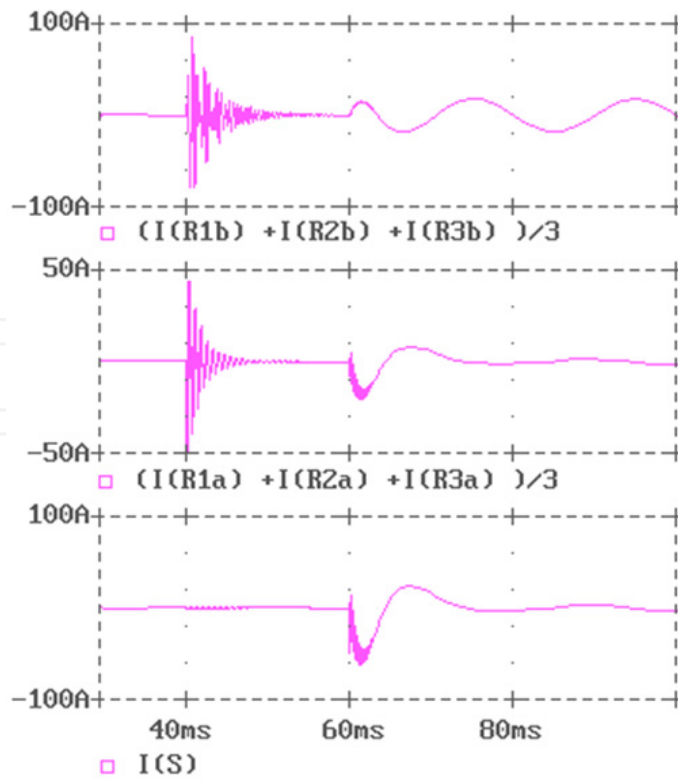
Figure 69. Time variation of the currents when MVN is at resonance, $R_t = 1\Omega$, $\alpha = 90°$, $C_{101a} = 9C_{102a}$
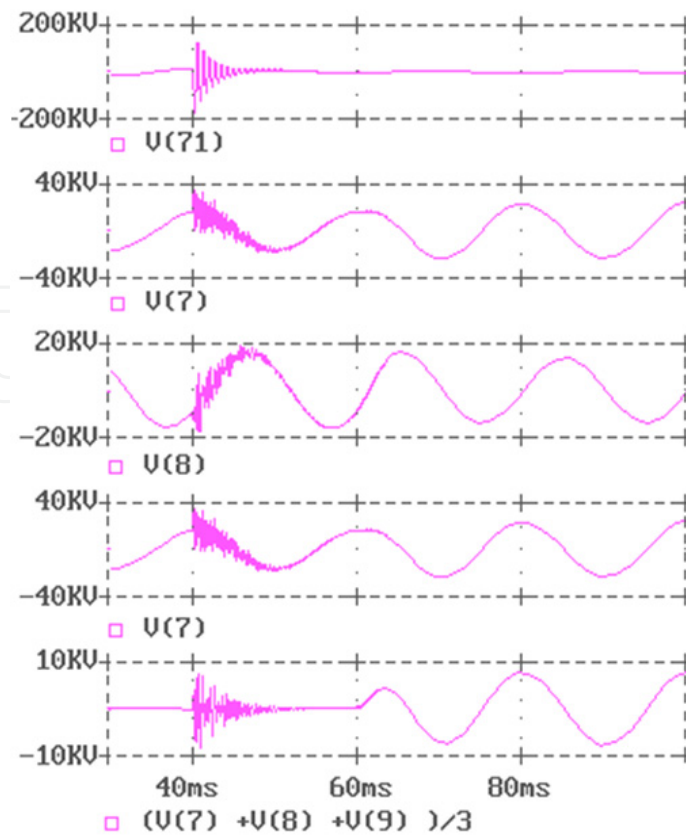
Figure 70. Time variation of the voltages, when MVN is at resonance, $R_t = 1\Omega$, $\alpha = 90°$, $C_{101a} = 9C_{102a}$
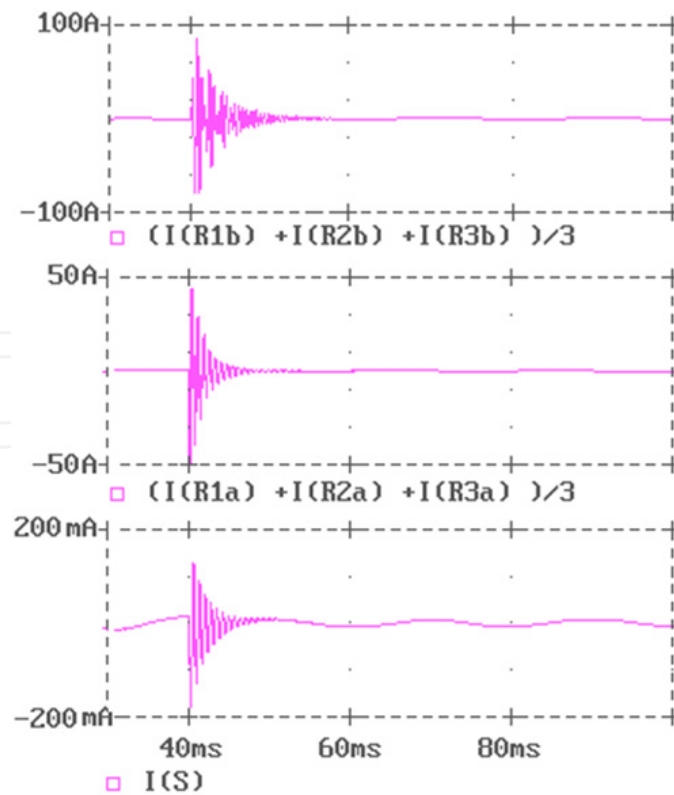
Figure 71. Time variation of the currents when MVN is at resonance, $R_t = 1M\Omega$, $\alpha = 90°$, $C_{101a} = 9C_{102a}$
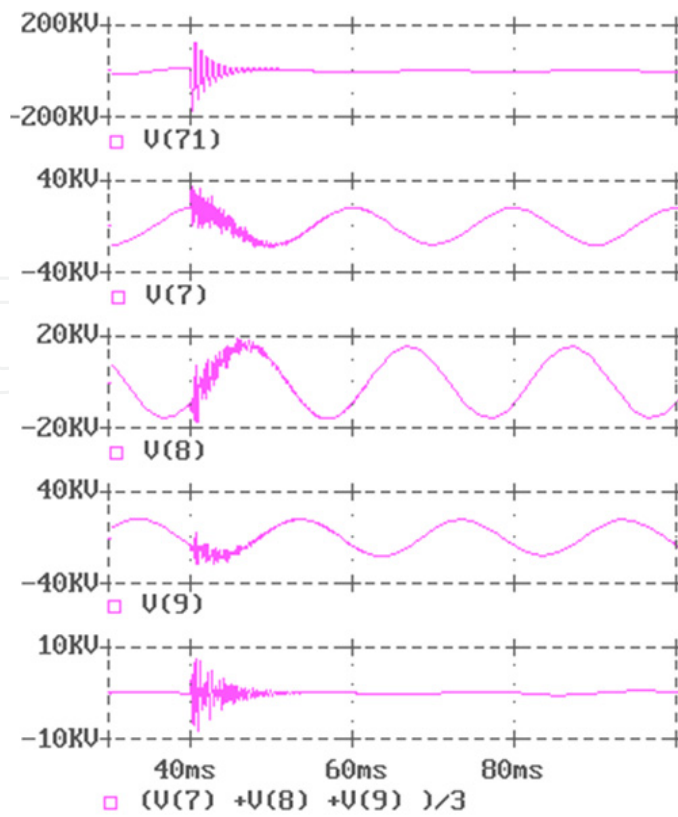
Figure 72. Time variation of the voltages. when MVN is at resonance, $R_t = 1M\Omega$, $\alpha = 90°$, $C_{101a} = 9C_{102a}$
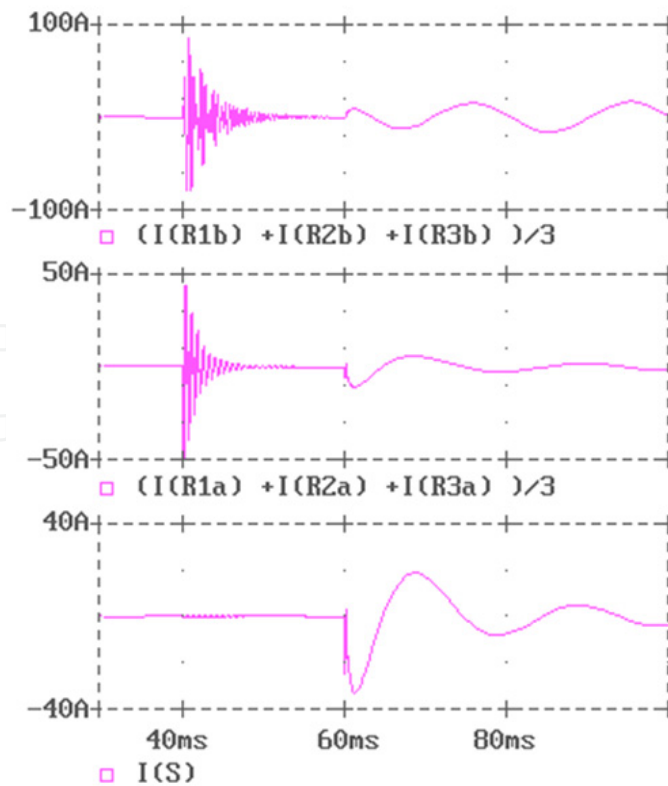
Figure 73. Time variation of the currents when MVN is at resonance, $R_t = 100\Omega$, $\alpha = 90°$, $C_{101a} = 9C_{102a}$
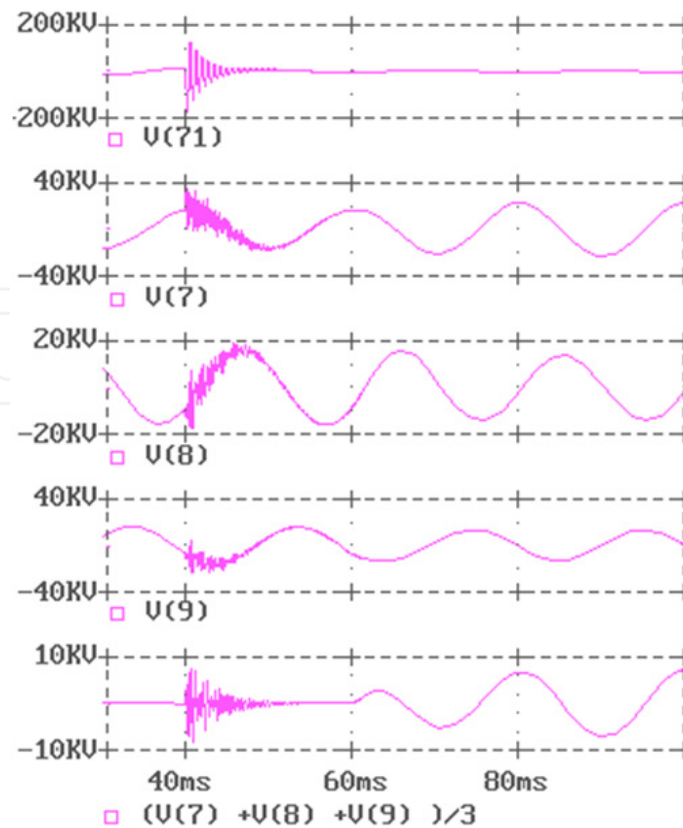
Figure 74. Time variation of the voltages, when MVN is at resonance, $R_t = 100\Omega$, $\alpha = 90°$, $C_{101a} = 9C_{102a}$

When $R_t = 1M\Omega$ the fault becomes of the type broken conductor and at t=60ms does not occur a transient regime.

When the fault is of the type interrupted conductor with ground contact towards the customer the heavyest situation is shown to be when the phase is near 90°.

For higher values of R_t the transient regime is less dangerous.

5. Measurement on real MVN

The results obtained during the measurements in the experiment area, while faults were produced on purpose, are shown in the followings.

The fault produced was of type single phase grounding.

The experimental aria contains 7 electric lines of 6kV, with total value of the capacitive current of 27A From the 7 electric linea 6 are connected at first system of bars and at the second bar system was connected the line on which the faults were produced. The capacitive current of this line is 2.7A.

The transformer station contains a transversal switch in connected position.

For recording the currents and the voltages during the experiment was used a CDR oscilloperturbograph.

Figures 75 to 83 show the following:

-   the zero sequence current of the faulty line $I^0_{PT\ Turn}$,
-   the current trough the compensation inductor I_B,
-   the star voltages, V_a, V_b, V_c; - the zerosequence voltage of MV bars from the transformer station U^0.

The experiment was made in order to verify the concordance with the numeric simulation and to validate the accuracy of the simulator.

The experiment consisted on producing on purpose faults of the type single-phase grounding, namely:

-   metallic grounding of a phase $R_t = 0$,
-   grounding through the passing resistance $R_t = 250\ \Omega$,
-   grounding through the passing resistance $R_t = 500\ \Omega$.

The functioning regimes of the MV network were:

-   MV network functioning at resonance; -MV network functions at 10% overcompensation,
-   MV network functions at 10% undercompensation.

The three recordings, corresponding to the three functioning regimes for metallic grounding are shown in Figs. 75, 76 and 77.
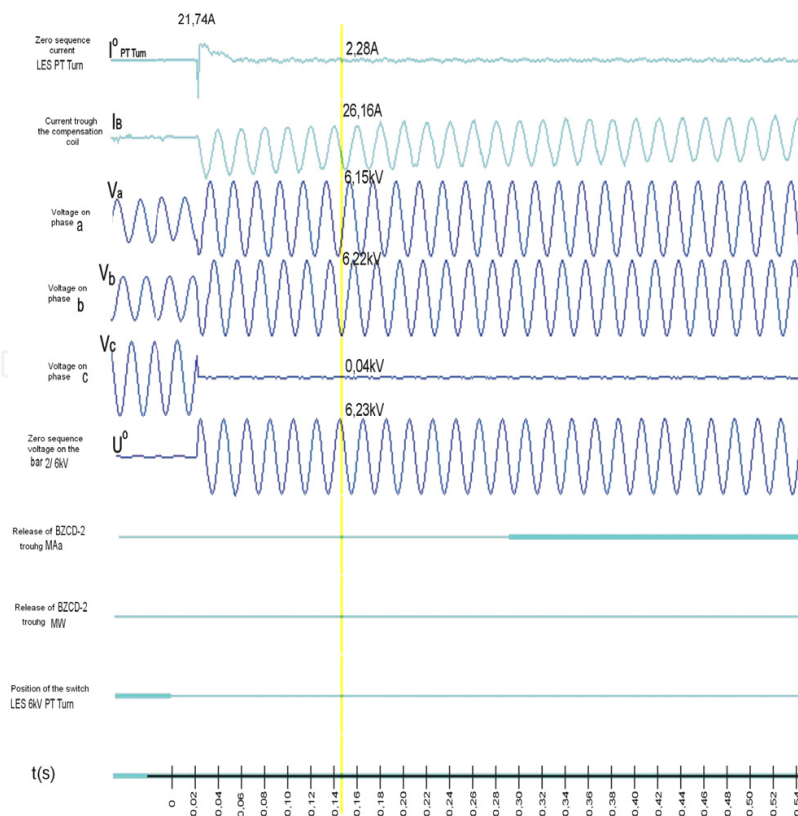
Figure 75. Single phase metallic grounding, $R_t = 5\ \Omega$, network at resonance
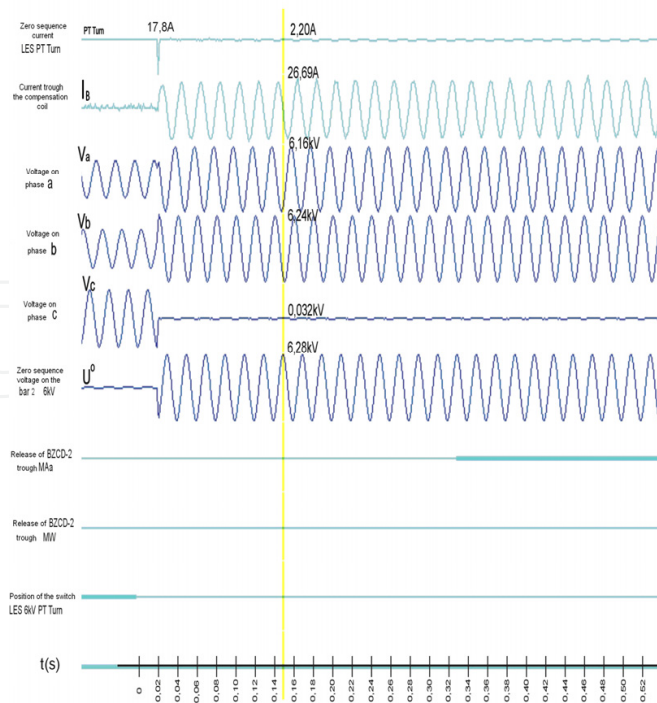
Figure 76. Single phase metallic grounding, Rₜ= 5 Ω, network at 10% over-compensation network
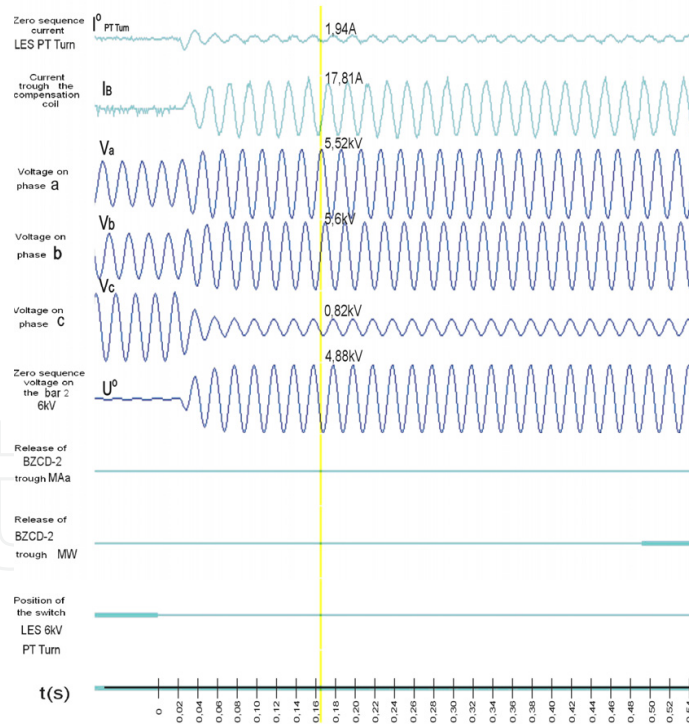
Figure 77. Single phase grounding with Rₜ=5 Ω, 10% under-compensated network

By comparing the shape of the current of the faulty line during the transient regime (the zero sequence current of the faulty line) obtained by numeric simulation with the one obtained by recording the same current during experiment it can be observed that the simulated current has an oscillating component greater than in recorded experiment.

This difference is due to a greater equivalent resistance of the experimental equivalent circuit than the simulated one.

In the same maner, as for the metallic grounding, but with a 250Ω grounding resistance for the three functioning regimes of the network the, results are presented in Figs. 78, 79 and 80.
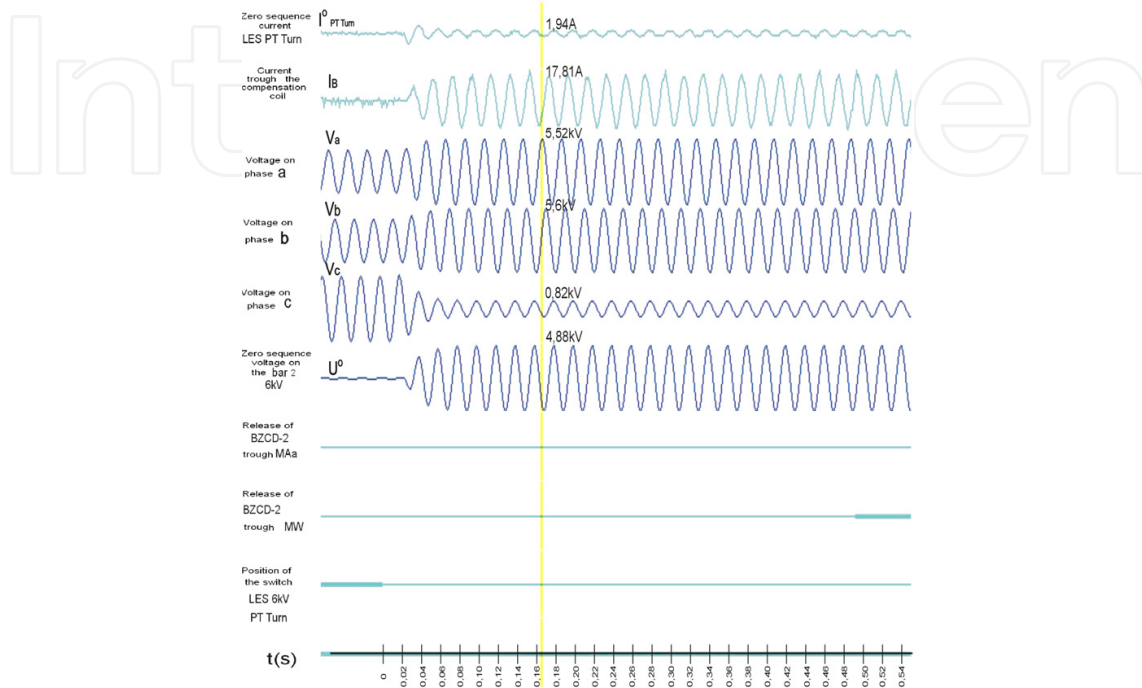
Figure 78. Single phase grounding with R_t=250 Ω, network at resonance
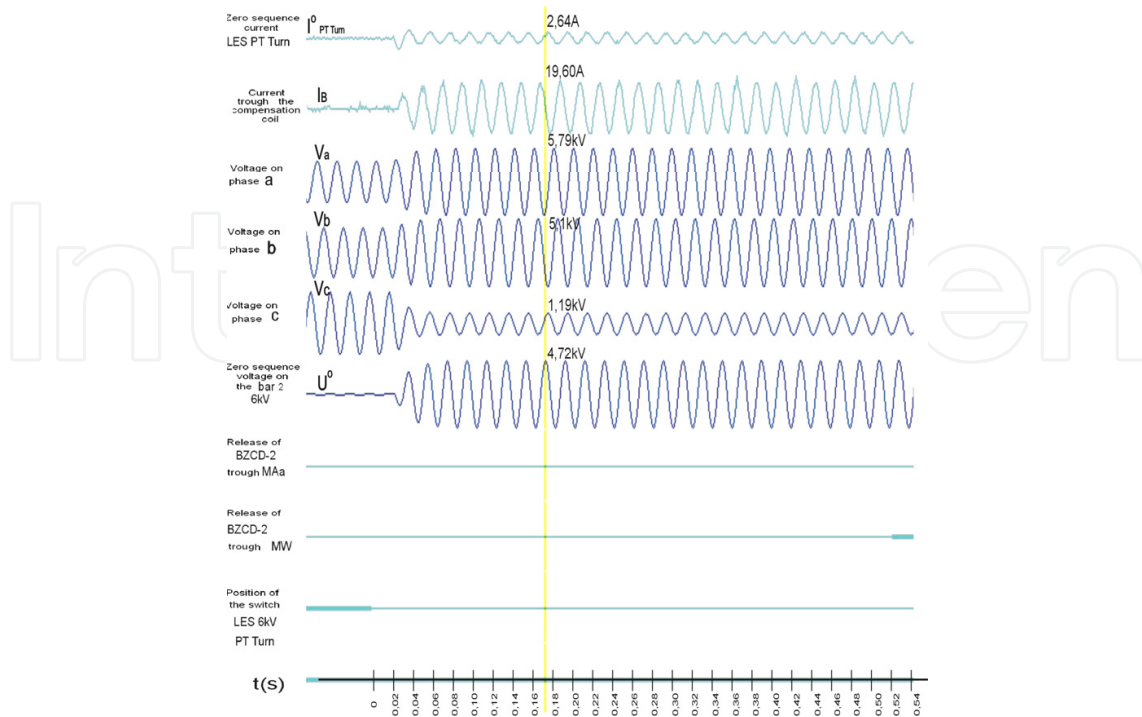
Figure 79. Single phase grounding with R_t=250 Ω, 10% over-compensated network
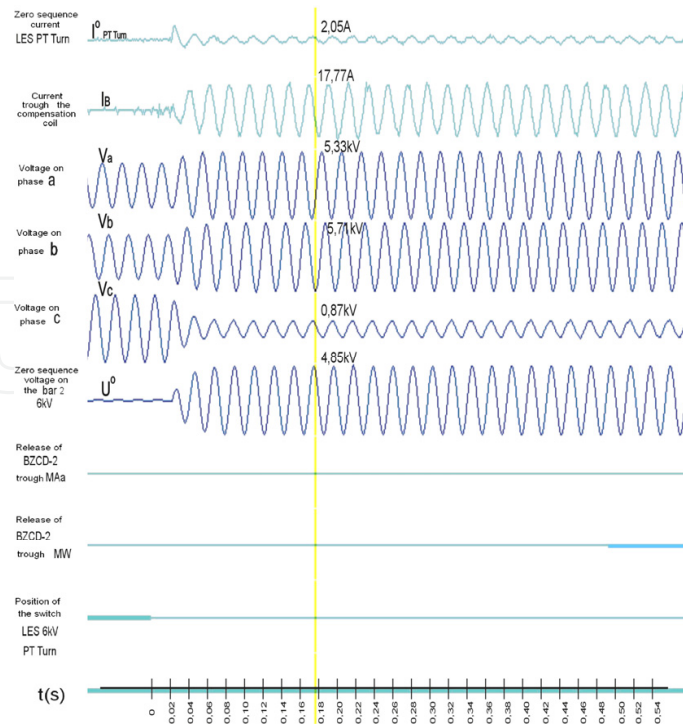
Figure 80. Single phase grounding with R$_t$=250 Ω, 10% under-compensated network

The third value for the grounding resistance used in the experiment is 500Ω and the results for the resonant regime, for 10% overcompensated and for 10% undercompensated are presented, respectively, in the figures 81, 82 and 83.
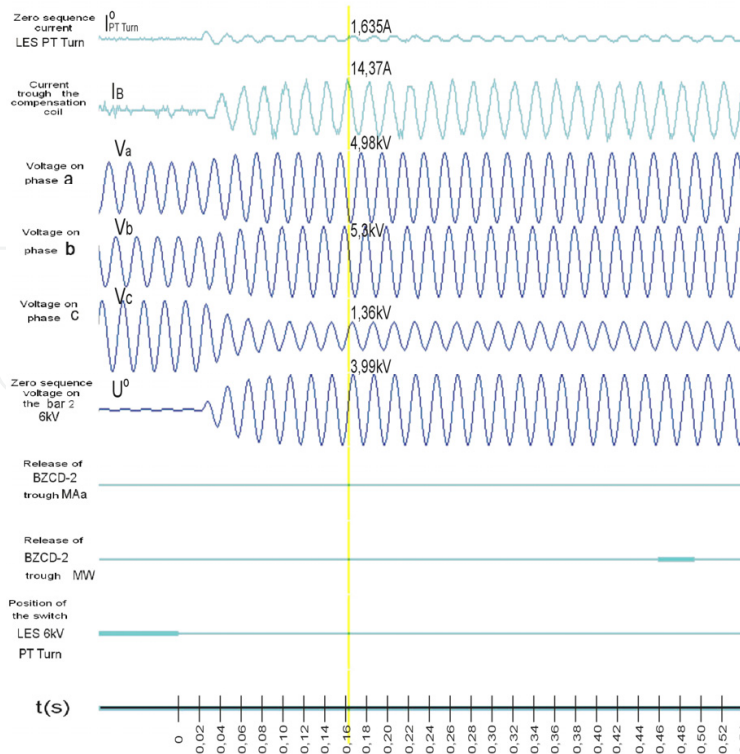
Figure 81. Single phase grounding resistance, R$_t$= 500 Ω, network at resonance
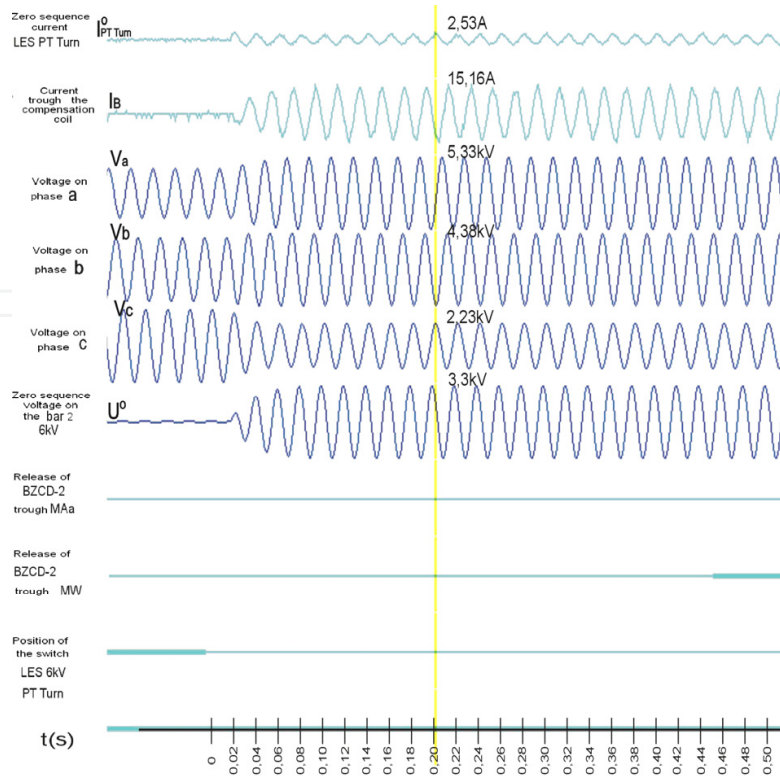
**Figure 82.** Single phase grounding resistance R$_t$= 500 Ω, network at 10% overcompensation
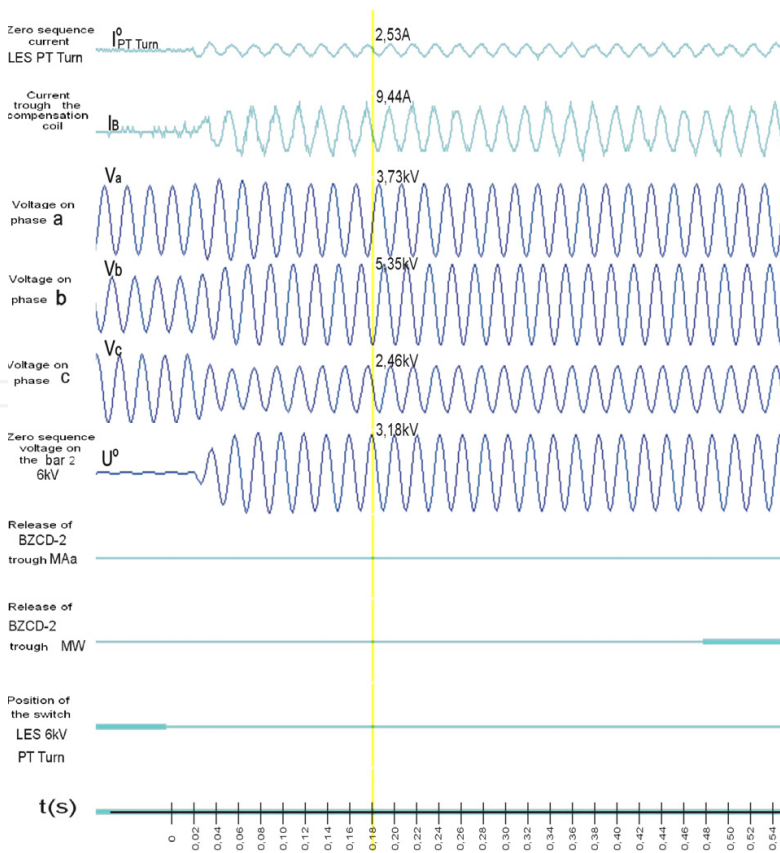
Figure 83. Single phase grounding with R$_t$=500 Ω network at 10% undercompensation

Table 1, campare some of the values measured during the experiment with the corresponding values obtained by numeric simulation.

The significance of the symbols from the table is as follows:

- I^0_{max} – maximal value of the zero sequence current on the faulty line,
- I_B – current trough the compensation inductor,
- I^0_{stab} – the zero sequence current of the faulty line, after the dumping of the dead-beat component,
- t_{am} – dumping time of the dead-beat component,
- U^0 – the zero sequence voltage at the MV bars of the transform station,
- U_f – voltage of the healty lines.

From Table 1. results that the differences between the values obtained by the numerical simulation and the values measured during the experiment are reasonably small.

Regime of the network	Symbol of quantities	$R_t[\Omega]$								
		5			250			500		
		Values obtained by		Error [%]	Values obtained by		Error [%]	Values obtained by		Error [%]
		Experi-ment	Simu-lation		Experi-ment	Simu-lation		Experi-ment	Simu-lation	
Resonance	$I^0_{max}[A]$	21,7	24,6	13,4	4,8	4,5	6,3	2,8	2,6	7,1
	I_B [A]	26,16	24,3	7,1	17,81	16,2	9,1	14,37	12,84	10,6
	$I^0_{stab}[A]$	2,28	2,42	6,1	1,94	1,75	9,8	1,64	1,49	9,1
	t_{am} [ms]	126	130	3,2	38	34	10,5	57	54	5,3
	U^0 [kV]	3,6	3,55	1,4	2,62	2,43	7,3	2,31	2,17	6,1
	U_f [kV]	6,22	6,03	3,1	5,6	5,46	2,5	5,3	4,78	9,8
10% Over-compensated	$I^0_{max}[A]$	17,8	58	226	4,2	4,5	7,1	3,2	2,9	9,4
	I_B [A]	26,69	24,82	7,0	19,6	18,3	6,6	15,16	13,86	8,6
	$I^0_{stab}[A]$	2,2	2,06	6,4	2,64	2,42	8,3	2,53	2,27	10,3
	t_{am} ms]	80	86	7,5	35	32	8,6	41	37	9,8
	U^0 [kV]	3,63	3,55	2,2	2,73	2,47	9,5	1,91	1,7	9,9
	U_f [kV]	6,24	5,96	4,5	5,69	5,21	8,4	4,38	4,76	8,7

Regime of the network	Symbol of quantities	$R_t[\Omega]$								
		5			250			500		
		Values obtained by		Error [%]	Values obtained by		Error [%]	Values obtained by		Error [%]
		Experiment	Simulation		Experiment	Simulation		Experiment	Simulation	
10% Under - compensated	$I^0_{max}[A]$	20,99	43	105	4,3	4,5	4,7	3,1	2,8	9,7
	$I_B[A]$	22,82	21,28	6,7	17,77	16,5	7,1	9,44	9,22	2,3
	$I^0_{stab}[A]$	2,5	2,32	7,2	2,05	1,91	6,8	2,53	2,31	8,7
	t_{am} ms]	198	210	6,1	31	28	8,6	23	21	8,7
	U^0 [kV]	3,59	3,56	0,84	2,8	2,53	9,6	1,84	1,67	9,1
	U_f [kV]	6,2	5,97	3,7	5,71	5,39	5,6	5,35	4,81	10,1

Table 1. Comparison of measured and simulated values

6. Conclusions

The numerical simulator designed by us allows the analysis of transients caused by diferent types of faults, such as simple groundings, double groundings, or broken conductor grounded towards the consumer.

We have compared results obtained by simulation with measured values only for simple grounding faults.

In this type of fault the simulator is validated by the measurements, no matter how the neutral point of the medium voltage network is grounded and whatever are the functioning conditions of the electrical network.

The results from Table 1. show that the simplificatory conditions, taken into account for developing the simulator, are correct.

The numerical simulation of the transient regimes caused by simple grounding faults produced in medium voltage networks shows to be an efficient method for analyzing such faults.

The most dangerous transient regimes occur when the initial phase of the voltage of the faulty line is near 90°.

The initial phase of the voltage, that happen to be in the very moment of producing the fault, was taken with the same value in simulation. The differences between the maximal

values of zero sequence component, obtained by the two methods, are quite acceptable from a technical point of view and this concordance validates the model.

The resistance of the broken conductor to ground is extremely important, small values of R_t implying long damping periods. If this undesirable condition happens the currents might have high values, as well as important values of the over voltages leading to important supplementary mechanical stress and damages of the insulating devices and, eventually a simple fault can turn to a multiple fault situation.

For small values of the grounding resistance at the fault location ($R_t < 10\Omega$) difference between measured and simulated values is a litle higher than in the case of greater values ($R_t > 100\Omega$).

The model is very useful by giving the values of the voltages on the healthy lines (over voltages that might jeopardize the insulation) and zero sequence currents of the faulty lines (fixing the condition of the fault detection by protection devices).

Using the conclusions of the simulation of a MVN for the values of the currents and voltages during different types of faults it is possible to adjust the prescribed values of the protection.

Simulation of the broken conductor fault, either connected to the ground or not, shows that resonance might occur, over voltages due to this resonances being dangerous to the equipments.

When double phase to ground fault was simulated the values of the voltages showed dangerous voltages for step or touch voltage.

The numerical simulator has the advantage of analyzing rapidly several variants as models of different possible situations.

The simulator is flexible and all kinds of faults can be simulated for different MVN, just by making the proper modification in the parameters of the simulator. These modifications are slightly easier to be performed when PSPICE simulating model is used.

Either using PSPICE or Mathlab-Simulink the accuracy of the analysis is similarly good.

The precision of the results obtained by simulation depends essentially on the accuracy of the MVN parameters.

Author details

Dumitru Toader, Stefan Haragus and Constantin Blaj
"Politehnica" University of Timisoara, Romania

7. References

Blume, W. (1986). *Computer Circuit Simulation*, BYTE, July 1986

Bucatariu, I. & Surianu, F. (2009). Optimal Placement of Fixed Series Capacitor in Distribution Networks, *Proceedings of the 9thWSEA/IASMES International Conference on*

Electric Power Systems High Voltages, Electric Machines Control & Signal Processing, Genova, Italy, October 17-19, 2009, pp.65-70

Chuco, B. (2005). Electrical Software Tools Overview *in* SINATEC-IEEE

Curcanu, G., Toader, D. & Pandia, T. (2006). Determination of overvoltages in high voltage networks at single phase faults by numarical simulation and experiments, *Proceedings 12th International IGTE Symposium,* Gratz

DeCarlo, R & Lin, P. (2001). *Linear Circuit Analysis,* Oxford University Press

Danyek, M., Handl, P.& Raisz, D. (2002). Comparison of Simulation Tools ATP-EMTP and MATLAB-Simulink for Time Domain Power System Transient Studies, *Proceedings of the European EMTP-ATP Conference,* Sopron, Hungary

Dessaint, L.-A., Al-Haddad, K., Le-Huy, H., Sybille, G. & Brunelle, P. (1999). *A power system simulation tool based on Simulink,* IEEE Trans. on Ind. Electronics, vol. 46, no. 6, pp. 1252-1254, Dec. 1999

Dommel, H.W. (1995). *ElectroMagnetic Transient Program. Theory Book,* Bonneville Power Administration, Portland

Drapela, J. (2009). Performance of a Voltage Peak Detection-Based Flichermeter, *Proceedings of the 8thWSEAS International Conference on Circuits, Systems, Electronics, Control & Signal Processing,* Teneriffe, Spain, December 14-16, 2009, pp.296-301

Foltin, M., Ernek, M. & Hnat, J. (2006). SimPowerSystems in Education, *Mezinarodni Konference Technical Computing,* Prague

Hasler, M. & Neirynck, J. (1985). *Circuits non lineares,* Presses Polytechniques Romandes, Lausannes.

Iordache, M. & Mandache, A. (2004). *Computer Aided Analyse of Nonlinear Circuits (in Romanian) ,* Politehnica Press Bucharest

Istrate, M., Gavrilas, M., Istrate, C. & Ursuleanu, R. (2009). Algorithms in Transmission Grids Using ATP Simulations, *Proceedings of the 9thWSEA/IASMES International Conference on Electric Power Systems High Voltages, Electric Machines Control & Signal Processing,* Genova, Italy, October 17-19, 2009, pp.109-114

Karlsson, A. (2005). *Evaluation of Simulink/SimPowerSystems and other Commercial Simulation Tools for the Simulation of Machine System Transient,* Swedish Royal Institute of Technology, Stockholm

Mandache, L. & Topan, D. (2009). *Algorithms for Electric Circuit Simulation,* Universitaria Press Craiova

Radoi , C. (1994). *SPICE Simulation and Analysis of Electronic Circuits,* Ameo Press Bucureşti.

Rashid, M.H. & Rashid, H.M. (2006) *SPICE for Power Electronics and Electric Power,* Taylor & Francis Group, Boca Raton

Ross, C.C. (2004). *Differential Equations,* Springer Science, pp.51-56

Sybille, G., Brunelle, P., Hoang Le-Huy, Dessaint, L.A. & Al-Haddad, K., (2000). *Theory and applications of power system blockset, a MATLAB/Simulink-based simulation tool for power systems,* Power Engineering Society Winter Meeting 2000, IEEE, Vol.1, pp.774-779

Vladimirescu, A. (1999). *SPICE*, Ed.Tehnica, Bucuresti

Vladimirescu, A. (1997) SIMULINK ; *Dynamic System Simulation for MATLAB, User's Guide, version 2.1*, MathWorks Inc.